Journal of Iberian Geology (2021) 47:121–150
https://doi.org/10.1007/s41513-020-00148-7

RESEARCH PAPER

Tectonic setting and isotopic sources (Sm–Nd) of the SW Iberian Autochthon (Variscan Orogen)

José Manuel Fuenlabrada[1] · Ricardo Arenas[2] · Rubén Díez Fernández[3] · José González del Tánago[2] · Luis Miguel Martín-Parra[3] · Jerónimo Matas[3] · Esther Rojo-Pérez[2] · Sonia Sánchez Martínez[2] · Pilar Andonaegui[2] · Byron Solis Alulima[2]

Received: 9 July 2020 / Accepted: 11 November 2020 / Published online: 2 January 2021

Abstract

Metasedimentary rock successions in Sierra Albarrana Group (SW Iberia Autochthonous Domain) were deposited during the Early Paleozoic influenced by the evolution of a peri-Gondwanan active margin. Their geochemical composition indicates dominant contributions from felsic igneous sources and an upper continental crust provenance. The high mineralogical and geochemical maturity, together with negative $\varepsilon Nd_{(530)}$, ranging from − 11.3 to − 4.5, and old Nd model ages (TDM: 1388–1897 Ma) imply reworked materials from old continental source areas with a limited juvenile contribution for the siliciclastic sedimentary rocks in Sierra Albarrana. Both, geochemical and isotope features were caused by the progressive denudation of rocks bearing the isotopic imprint from an old basement exposed along the Gondwanan margin. The paleobasin for the SW Iberia Autochthon probably occupied an outboard position across the peri-Gondwanan margin during Ediacaran–Cambrian times. In a convergent scenario, the interaction between the peri-Gondwanan trench and the external part of the continent generated tectonic uplift, giving way to exposure of crust formed during earlier stages of the Cadomian Orogeny and erosion. Sediment redistribution through Early Paleozoic times supplied recycled detrital materials, which likely filled a retro-arc basin formed after the switch from an extensional to a compressional regime in the upper plate of the Cadomian Orogen that is recorded throughout the peri-Gondwanan domain of Iberia. A subsequent extensional stage led to a progressive widening of its marginal basins, thus bringing the onset of a passive margin from the Cambro–Ordovician onwards. Nd model ages of the Sierra Albarrana Group overlap those of Early Cambrian series from the southernmost Central Iberian Zone, and are considered an indication for the paleogeographic closeness between all these sequences during Cambrian times, occupying eastern positions closer to Tuareg Shield and the Sahara Metacraton sections along the Gondwanan margin.

Keywords Iberian massif · Sm–Nd isotope geochemistry · SW autochthonous domain · Sierra Albarrana Group · Gondwanan paleogeography

Resumen

Las series de rocas metasedimentarias en el Grupo Sierra Albarrana (Dominio Autóctono del SW de Iberia) se depositaron durante el Paleozoico Inferior, influidas por la evolución de un margen activo peri-Gondwánico. Su composición geoquímica indica una contribución dominante desde fuentes ígneas félsicas con afinidad con una corteza continental superior. La elevada madurez mineralógica y geoquímica, junto con valores negativos de εNd(530) (− 11.3 a − 4.5) y edades modelo de Nd relativamente antiguas (TDM: 1388–1897 Ma), implica materiales retrabajados desde áreas fuente continentales antiguas, con una contribución juvenil limitada para las rocas siliciclásticas estudiadas en el Grupo Sierra Albarrana. Sus características geoquímicas e isotópicas fueron fruto de una denudación progresiva de rocas con una composición isotópica

Electronic supplementary material The online version of this article (https://doi.org/10.1007/s41513-020-00148-7) contains supplementary material, which is available to authorized users.

✉ José Manuel Fuenlabrada
jmfuenla@ucm.es

Extended author information available on the last page of the article

afín a un basamento antiguo expuesto a lo largo del margen de Gondwana. Teniendo en cuenta la información disponible para el SW del Macizo Ibérico, la paleocuenca del Dominio Autóctono del SW de Iberia probablemente ocupó posiciones externas en el margen peri-Gondwánico durante la transición Ediacárico-Cámbrico. En un contexto de convergencia, la interacción entre la trinchera peri-Gondwánica y la parte externa del continente ocasionó probablemente un levantamiento tectónico pronunciado, dando lugar a la exposición y posterior erosión de la corteza continental peri-Gondwánica formada durante las etapas iniciales de la Orogenia Cadomiense. La redistribución de sedimentos durante el Paleozoico Inferior aportó materiales detríticos reciclados, que probablemente rellenaron una cuenca retro-arco, formada tras el cambio de un régimen compresivo a uno extensional en la placa superior del Orógeno Cadomiense y que se registra a lo largo de todo el dominio peri-Gondwánico de Iberia. El avance en la extensión condujo a un progresivo ensanchamiento de las cuencas marginales, marcando el inicio de un margen pasivo desde el periodo Cambro-Ordovícico en adelante. Las edades modelo de Nd del Grupo Sierra Albarrana se solapan con las obtenidas en series del Cámbrico Inferior del sur de la Zona Centro Ibérica, y se consideran indicadoras de una cercanía paleogeográfica entre estas secuencias durante el Cámbrico, ocupando posiciones relativamente orientales, cercanas al Escudo de Tuareg y al Metacratón del Sahara.

Palabras clave Macizo Ibérico · Geoquímica isotópica Sm–Nd · Dominio Autóctono del SW · Grupo Sierra Albarrana · Paleogeografía de Gondwana

1 Introduction

In the latest years, many works have focused on understanding the magmatic and tectonic events that took place during the Neoproterozoic and Early Paleozoic in the peri-Gondwanan magmatic arc-systems related to the Cadomian Orogeny (e.g., Murphy and Nance 1989; Ballèvre et al. 2001; Linnemann and Romer 2002; von Raumer et al. 2002; Pereira et al. 2006;Linnemann et al. 2014; Andonaegui et al. 2016; Arenas et al. 2018; Díez Fernández et al. 2019). This effort has gone hand by hand with an aim to deciphering the relative position of Variscan terranes along the paleomargin of Gondwana before its Devonian collision against Laurussia, figuring out in the way the paleogeography of the Ediacaran paleomargin of Gondwana (e.g., Díez Fernández et al. 2010; Ábalos et al. 2012; Avigad et al. 2012; Pereira et al. 2012a, 2020; Fernádez Suárez et al. 2014; Stephan et al. 2019a, b; Fuenlabrada et al. 2020). Geochemical, isotopic and geochronological approaches have become highly important to identify the provenance of the Iberian terranes. U–Pb–Hf geochronology and isotope geochemistry in detrital zircons have grown into a useful mean in providing paleogeographic models for their Gondwanan provenance (e.g., Fernández-Suárez et al. 2000, 2003, 2014; Ugidos et al. 2003a; Pereira et al. 2008, 2012a; Bea et al. 2010; Díez Fernández et al. 2010; Ábalos et al. 2012; Talavera et al. 2012; Albert et al. 2015; Orejana et al. 2015; Hernderson et al. 2016) and for constraining the tectonothermal history and the particular provenance of correlative European terranes (e.g., Linnemann et al. 2007; Drost et al. 2011; Avigad et al. 2012, 2018; Abbo et al. 2015; Arenas et al. 2016a; Collet et al. 2020; Martínez Catalán et al. 2020).

Together with the development of U–Pb–Hf geochronological and isotope geochemistry tools, whole-rock geochemistry and Nd-isotope composition studies in metasedimentary rock sequences have provided new data to improve the understanding about the provenance and the probable depositional environment of the Iberian metasedimentary record (e.g., Nägler et al. 1995; Ugidos et al. 2003b; López-Guijarro et al. 2008; Bea et al. 2010; Fuenlabrada et al. 2010, 2012, 2016; Pastor-Galán et al. 2013; Fernández-Suárez et al. 2014; Villaseca et al. 2014; Díez Fernández et al. 2017; Rojo-Pérez et al. 2019). An extensive sedimentary record in the Iberian Massif has allowed the study of the late Ediacaran evolution of a peri-Gondwanan active margin and its subsequent transition to a passive margin during Cambrian–Ordovician times (Rodríguez-Alonso et al. 2004b; Pereira et al. 2006; Linnemann et al. 2008; Sánchez-García et al. 2008, 2014; Fuenlabrada et al. 2020). Geochemical and Nd-isotope data from Iberian terranes have provided evidence for changes in the depositional settings by that time. The filling of a peri-Gondwanan back-arc basin, strongly influenced by ongoing magmatic activity, occurred during Ediacaran times (Fuenlabrada et al. 2012, 2016; Pereira et al. 2012a; Fernández-Suárez et al. 2014). The subsequent widening of that basin during the Early Cambrian period led to a change in the siliciclastic contributions to more recycled and older detritus (Fuenlabrada et al. 2020). The Nd-isotope information from siliciclastic series of the Iberian Massif represents an effective and comparative method for paleoreconstructions of the current Iberian terranes during the Neoproterozic and Paleozoic times (Fernández-Suárez et al. 2014a; Albert et al. 2015; Cambeses et al. 2017; Fuenlabrada et al. 2020), allowing a comparison between tectonostratigraphic units, members of the same terrane, but currently dispersed over the Iberian Massif due to superimposed deformation.

The current disposition of domains in the Iberian Massif was the result of the Pangea assembly during the Devonian through to the Carboniferous period after the closure of the

Rheic and other oceanic basins (Franke 1989; Matte 1991; Winchester et al. 2002; von Raumer et al. 2003; Nance et al. 2010; Stampfli et al. 2013). The collision between Gondwana and Laurussia raised the Variscan Orogen (Fig. 1a), which is featured by suture zones and far-traveled (allochthonous) terranes that spread over the Iberian Massif and onto autochthonous sections of the margin of Gondwana (Fig. 1b) (Martínez Catalán et al. 1997, 2007; Ribeiro et al. 2007; Simancas et al. 2009; Arenas et al. 2014, 2016a; Díez Fernández and Arenas 2015; Díez Fernández et al. 2016). The generally accepted criterion for defining the autochthonous character of Iberian terranes has been their lower (plate) structural position relative to Variscan suture zone exposures (e.g., Ries and Shackleton 1971; Arenas et al. 1986, 2016a; Simancas et al. 2009; Martínez Catalán et al. 2020 and references therein). This is many times accompanied by a particular metamorphic evolution during the Variscan accretionary history, which makes them different from the Iberian allochthonous sections, i.e., a Barrovian-type evolution and a usual lack of high-P metamorphism (Dallmeyer et al. 1997; Martínez Catalán et al. 2009; Díez Fernández et al. 2016). The autochthonous sections represent inboard domains of the North African margin of Gondwana and include pre-Variscan metasedimentary sequences that range between Ediacaran and Devonian in age (Alvarez Nava et al. 1988; Gutierrez-Marco et al. 1990; San José et al. 1990; Valladares et al. 2000, 2002; Rodríguez Alonso et al. 2004a).

Here we present a new comprehensive whole-rock and Nd-isotope geochemical data set from the metasedimentary rocks cropping out in an autochthonous section of the SW Iberian Massif, locally referenced to as the Sierra Albarrana

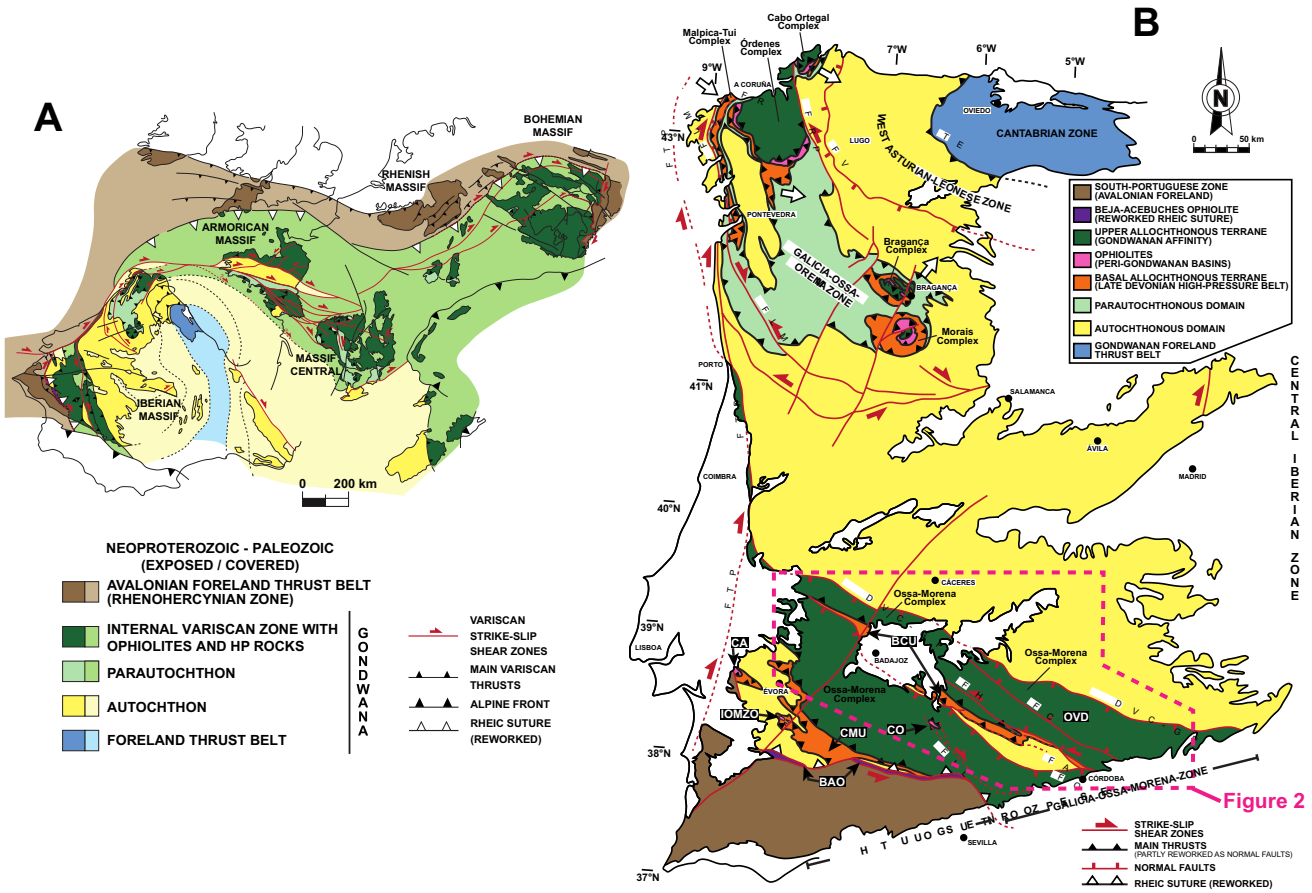

Fig. 1 **a** Zonation of the Variscan Orogen (Díez Fernández and Arenas 2015; Arenas et al. 2016b). **b** Geological map of the Iberian Massif showing the distribution of autochthonous and allochthonous terranes in NW and SW Iberia (Díez Fernández and Arenas 2015). Location of the geological map presented in Fig. 2 is shown. *AF* Azuaga Fault, *BAO* Beja-Acebuches Ophiolite, *CA* Carvalhal Amphibolites, *CF* Canaleja Fault, *CMU* Cubito-Moura Unit, *CO* Calzadilla Ophiolite, *CU* Central Unit, *ET* Espina Thrust, *HF* Hornachos Fault, *IOMZO* Internal Ossa-Morena Zone Ophiolites, *LLF* Llanos Fault, *MLF* Malpica-Lamego Fault, *OF* Onza Fault, *OVD* Obejo-Valsequillo Domain, *PG-CVD* Puente Génave-Castelo de Vide Detachment, *PRF* Palas de Rei Fault, *PTF* Porto-Tomar Fault, *RF* Riás Fault, *VF* Viveiro Fault

Group. Major and trace elements showing low-mobility characteristics during weathering, sedimentary transport, and post-depositional processes, would provide clues to track the influence of the geodynamic frame over the development and evolution of the sedimentary basins in which the sedimentary protoliths of the Sierra Albarrana Group were deposited. Similarly, this geochemical and isotope approach would contribute to constrain the provenance and relative paleoposition of this autochthonous section of the Variscan Orogen relative to other peri-Gondwanan terranes of the Iberian Massif, with particular focus on other autochthonous sequences of the Iberian Variscides that are now exposed in the southernmost section of the Central Iberian Zone (Fuenlabrada et al. 2016), i.e., the closest ones to the study case.

2 Geological setting

The first division of the Iberian Massif made by Lotze (1945) and Julivert et al. (1972) resulted in several geotectonic zones (Cantabrian, West Asturian-Leonese, Central Iberian, Ossa-Morena, and South-Portuguese zones). They show particular stratigraphic, structural, magmatic and metamorphic features, defining external or more internal domains within the southernmost section of the Variscan Orogen (Fig. 1a) (Martínez Catalán et al. 2009; Simancas et al. 2009; Arenas et al. 2014; Díez Fernández et al. 2016). After that initial division, several authors have contributed with new data and perspectives towards a further discrimination of geotectonic zones (e.g., Galicia-Trás-os-Montes Zone; Farias et al. 1987). Certain domains that constitute these geotectonic zones preserve particular characteristics from the earlier Variscan orogenic imprint, tightly connected to continental subduction (Fernández-Suárez et al. 2002a; Stampfli et al. 2002; Martínez Catalán et al. 2009; Kroner and Romer 2013; Rubio Pascual et al. 2013; Albert et al. 2015; Arenas et al. 2016a). Devonian high-P metamorphism and/or peri-Gondwanan paleoposition are typical features for the terranes that are thrust onto inboard sections of Gondwana in Iberia, the latter being the autochthon to a suture zone and its upper plate that can now be observed as allochthonous dismembered pieces over the Iberian Massif (Díez Fernández and Arenas 2015). This allochthonous–autochthonous pair is the essence to the distinction of allochthonous complexes in NW Iberia, and can be also observed in the SW of the Iberian Massif. As a result, most of the former Ossa-Morena Zone emerged as a new allochthonous complex, composed by terranes with different origin and tectonothermal evolution, while the sections underlying this complex became part of the Iberian Autochthon (Fig. 1b; Díez Fernández and Arenas 2015).

The Ossa-Morena Complex preserves typical features for a North Gondwanan margin provenance (López-Guijarro et al. 2008, 2012b; Pereira et al. 2008; Rojo-Pérez et al. 2019), with a pre-Variscan (Ediacaran to Devonian) metasedimentary and metaigneous record (Fig. 2). The Cadomian tectonothermal history is linked to the geodynamic activity of a peri-Gondwanan continental arc during Ediacaran and Cambrian times (Eguíluz et al. 2000; Pereira et al. 2006; Linnemann et al. 2008; Díez Fernández et al. 2017, 2019; Arenas et al. 2018; Rojo-Pérez et al. 2019). In that context, the Ediacaran metasedimentary rocks constituting the so-called Serie Negra Group (Carvalhosa 1965) define the basal part of an upper allochthonous terrane (Díez Fernández and Arenas 2015; Arenas et al. 2016b; Díez Fernández et al. 2016), and although it appears widely throughout the complex, it is especially important in the central area of the Olivenza-Monesterio antiform (Eguiluz 1987; Quesada et al. 1990) (Fig. 2). The Serie Negra Group has been traditionally divided into the Montemolín and Tentudía formations (Eguiluz 1987). Occupying the lower part of the series, the Montemolín Formation is mainly composed by metasandstones (including black quartzites), mica-schists, and abundant intercalations of metabasites. The maximum depositional age for this formation has been estimated at 591 ± 11 Ma (U–Pb in detrital zircons; Ordoñez Casado et al. 2009). The protoliths of this formation have been interpreted as related to a passive margin setting (Quesada 1990; Cambeses et al. 2017), although their geochemical composition suggests the influence of a Cadomian volcanic arc during their sedimentation (López Guijarro 2006; Rojo-Pérez et al. submitted). The Tentudía Formation, as well as the Don Alvaro and Oliva de Mérida Successions (Bandrés et al. 2001), rest on top and includes metagreywackes, black metapelites, black quartzites and felsic metaigneous rocks and minor metabasites. The study of U–Pb in detrital zircons from the sedimentary protoliths of this formation yielded a maximum depositional age of 560–544 Ma (Schäfer et al. 1993; Ordóñez-Casado et al. 1998; Fernández Suárez et al. 2002b; Linnemann et al. 2008), with a probable deposition linked to the evolution of a back-arc basin (Bandrés 2001; Cambeses et al. 2017; Rojo-Pérez et al. 2019, submitted). Overlying discordantly, the volcanoclastic Malcocinado Formation (Fricke 1941), with igneous intrusions (El Escribano, El Mosquil, La Bomba; Sánchez Carretero et al. 1989), probably contains the boundary between Ediacaran and Cambrian times (Pereira 2015), while the discordant sequences of the Torreárboles Formation, mainly composed by metasandstones and metaconglomerates, have been attributed to the Early Cambrian (Liñan and Palacios 1983; Liñan 1984; Liñan et al. 1984). The Central, Cubito-Moura, and Escoural units (Fig. 1b) are members of a terrane that is located at the base of the allochthonous nappe pile (Basal Allochthonous Units), i.e., underlying the upper allochthonous terrane cited above (Uppermost Allochthonous Units) and on top of the Autochthon to the Ossa-Morena Complex

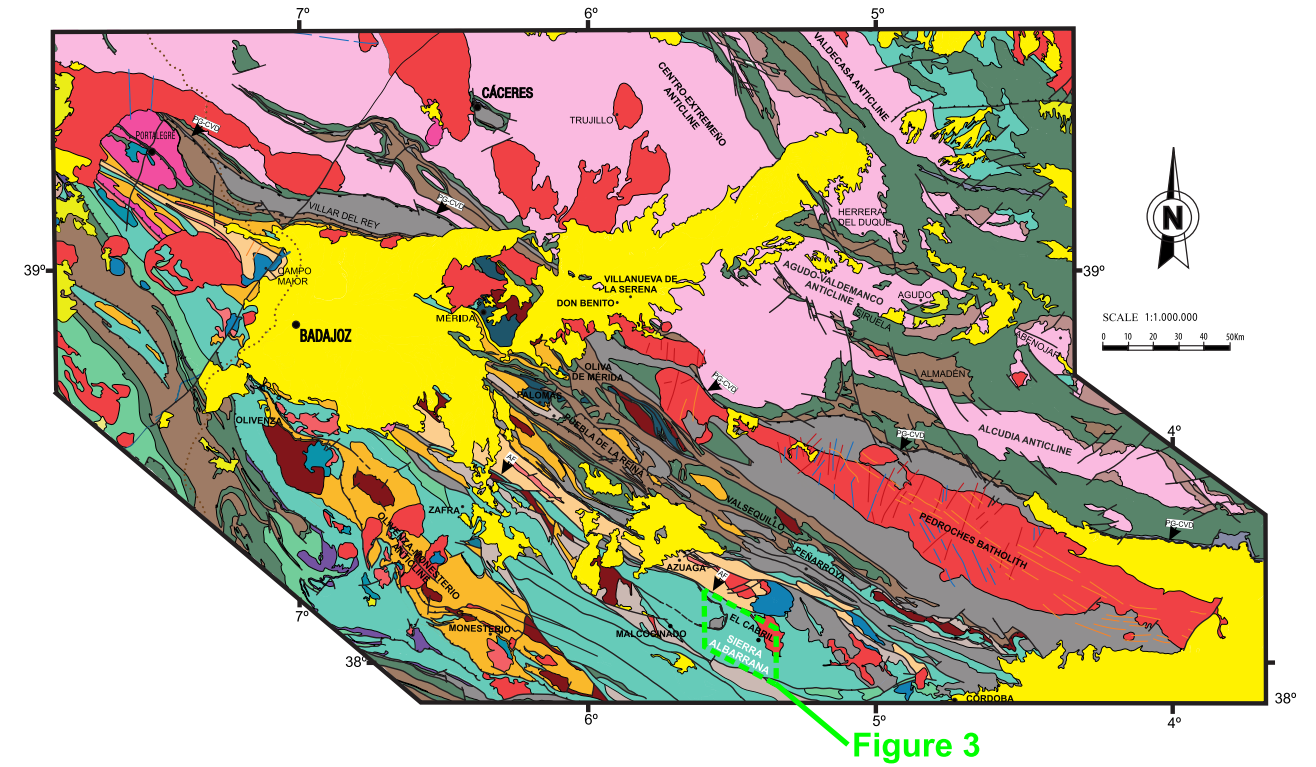

Fig. 2 Geological map of the Central Iberian Zone–Ossa-Morena Complex boundary (Rojo-Pérez et al. 2019; Based on the 1:1.000.000 geological map of Spain and Portugal, IGME 2015). *AF* Azuaga Fault, *PG-CVD* Puente Génave-Castelo de Vide Detachment. Location of the geological map and cross-section presented in Fig. 3 is shown

(Fig. 1b). The three of them, especially the Central Unit, have continental crust affinity, peri-Gondwanan provenance (Díez Fernández et al. 2017) and experienced Devonian high-P metamorphism (Moita et al. 2005; Abati et al. 2018).

The Sierra Albarrana Group (Delgado Quesada 1971; Garrote 1976; Azor 1994; González del Tánago 1995) is exposed immediately to the SW of the Badajoz-Córdoba Shear Zone, classically considered as the boundary between the Ossa-Morena Zone and the southernmost section of the Central Iberian Zone (Robardet 1976; Martínez Poyatos 1997; Pérez Estaún et al. 2004) (Fig. 2), where a dip-slip Variscan extensional fault is presented (Martín Parra et al. 2006). The best exposures of the Sierra Albarrana Group are located to the south of the Azuaga Fault (Chacón et al. 1974; Delgado Quesada et al. 1977; Apalategui et al. 1985; Ábalos et al. 1990), and resting under the Central Unit as an autochthonous section of the Variscan Orogen (Azor 1994; and references therein). According to González del Tánago and Peinado (1990), the tectonometamorphic evolution of this group defines it as a NW–SE elongated thermal dome, dominated by metasedimentary rocks and minor metabasites, folded into an antiformal structure. The Sierra Albarrana Group is composed mainly of four different lithostratigraphic successions, with a

dominant siliciclastic character, from bottom to top: (i) Albarrana Succession (AS), (ii) Cabril-Peña Grajera Succession (CGS), (iii) Albariza-Bembézar Succession (ABS), and (iv) Azuaga Formation (AzF) (Fig. 3).

González del Tánago y Peinado (1990) included the first two aforementioned units into a single one (Albarrana Gneisses Unit) that occupies the core of the antiformal structure, and consisting of rocks fairly different from the dominant schistose or phyllitic nature of the rocks in the rest of the units. The Albarrana Succession [also named as Albarrana Quartzites or Albarrana Formation by Delgado Quesada (1971) and Garrote et al. (1980), respectively] occupies the central area of the dome structure and it is mainly composed of quartzites (mainly feldspathic), paragneisses, with minor schists, migmatites, pegmatitic bodies and lenses of amphibolite. The paragneisses are essentially meta-arkoses with a predominant monotonous quartz-feldspathic composition (González del Tánago 1995). The Cabril-Peña Grajera Succession rests on top of the Albarrana Succession and consists mainly of paragneisses, migmatites, fine-medium grain sized metasandstones, feldspathic quartzites and minor schists, most of which derive from semipelitic and pelitic protoliths. This unit corresponds to the Blastomilonitic Formation and Cabril-Peña Grajera Formation defined by Delgado Quesada (1971) and Garrote et al. (1980), respectively, and Insúa et al. (1990) distinguished an additional member made of paragneisses and schists referred to as the Cerro Pavillos Succession (Fig. 3). The gneisses and migmatites of this unit are characterized by penetrative tectonic banding defined by quartz-feldspathic and biotite-rich layers (Azor 1994). The metasedimentary rocks so far described preserve primary sedimentary structures such as ripples and cross-bedding, and were considered as intertidal deposits with an important contribution from felsic volcanic sources by González del Tánago (1995; and references therein).

The Albariza-Bembézar Succession (Albariza-Bembézar Schist Unit; González del Tánago 1995) rests on top of the Cabril-Peña Grajera Succession (Fig. 3). Despite being divided into two formations according to their position in the NE or SW limb of the antiformal structure of the region (La Albariza and Bembézar formations; Delgado Quesada 1971; Garrote et al. 1980), their lithostratigraphic similarity, lateral structural continuity and metamorphic homogeneity were taken as solid grounds to merge them into a single succession, which may show some local minor differences regarding the abundance in amphibolite layers, pegmatites, or in the size of staurolite and garnet porphyroblasts (Insúa et al. 1990; González del Tánago 1995). This unit is mainly composed by a metapelitic succession of schists, amphibolite lenses, garnet-bearing amphibolites (Gónzalez del Tánago and Arenas 1991), interbedded with minor metasandstones and white quartzites, and dykes of diabase. Pegmatitic bodies can be found close to the contact with the Albarrana Succession, where it shows higher strain and incipient migmatization.

The Azuaga Formation mantles the antiform structure of the study area and occupies the upper structural position within the Sierra Albarrana Group (Fig. 3). The Azuaga Formation is separated from the so-called Central Unit (Azor et al. 1994) (Fig. 1b) by the Azuaga Fault, and from the rest of the Ossa-Morena Complex to the SW by the Onza and Malcocinado faults (Azor 1994). However, materials that can be correlated with those found in the Albariza-Bembézar Succession, and mainly in Azuaga Formation are found in a thrust sheet located to the north of the Central Unit (Fig. 2). The current juxtaposition of this unit onto the rest of the Sierra Albarrana Group was interpreted to have been carried out by the Casa del Café Fault (Azor 1994). The Azuaga Formation shows low-grade metamorphism, and consists of fine-grained metasedimentary sequences with turbiditic origin, mainly composed of characteristic laminated slates, as well as phyllites, minor quartzite intercalations, post-metamorphic dykes of diabase and some mica-schists towards the lower part of the series (González del Tánago 1995). The Cardenchosa pluton intruded this unit and produced contact metamorphism in its host (Insúa et al. 1990). This pluton is affected by Variscan deformation (Simancas et al. 2000), has been dated at Early Ordovician and interpreted as part of a late-rift episode, related to the Cambrian–Ordovician rift stage of the Iberian Massif (Azor et al. 2016; Sánchez García et al. 2019).

The successions here described were affected by several phases of deformation (Dallmeyer and Quesada 1992,2012; Azor et al. 2004). Earlier deformation was accompanied by intermediate-P metamorphism, which evolved to lower-P conditions in the whole set and to higher-T conditions towards the lower structural section (González del Tánago and Peinado, 1990). This gave rise to a normal metamorphic zonation from the biotite zone on top up to partial melting conditions towards the bottom (Garrote 1976; González del Tánago 1995). The penetrative metamorphic fabrics formed in this area were considered as formed in relation to a ductile shear zone (Azor and Ballèvre 1997), while the upright folds that affect the series were interpreted as Variscan and related to strike-slip shear zones (Simancas et al. 2000).

The age of the successions in Sierra Albarrana has been traditionally attributed to Precambrian times (Delgado Quesada 1971; Garrote 1976; Garrote et al. 1980; Quesada et al. 1990; López-Guijarro et al. 2008), although a correlation between the quartzites in the Albarrana Succession and the Ordovician Armorican Quartzite of the Central Iberian Zone was made by Apalategui et al. (1985). In the quartzites of the Albarrana Succession, ichnofossils, such as *Monocraterion*, suggest sedimentation in a shallow marine environment from Early Cambrian times onward (Azor et al. 1991; Marcos et al. 1991). López-Guijarro et al. (2008) ruled out

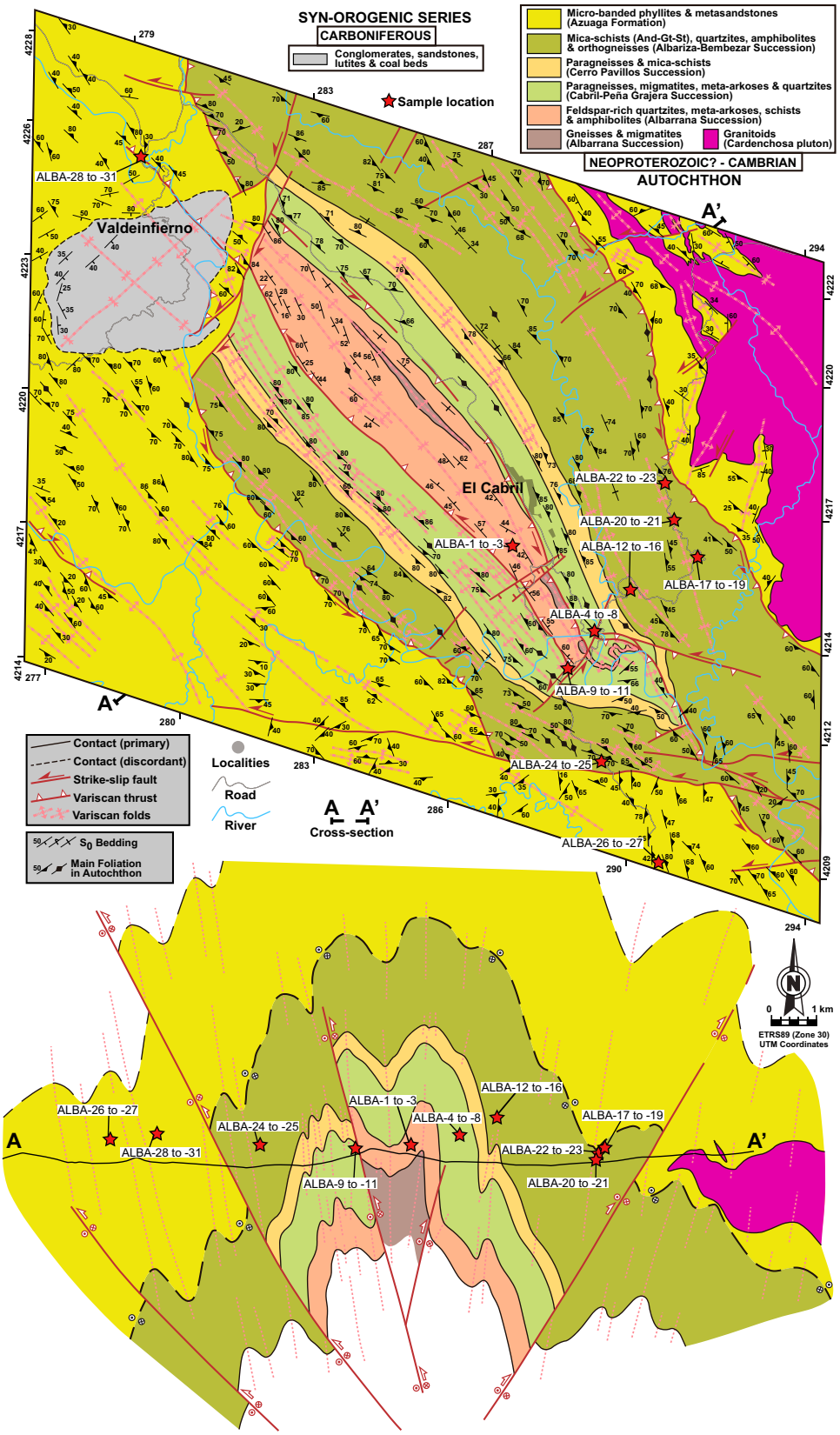

Fig. 3 Geological map and cross-section of the Sierra Albarrana Group (based on Insúa et al. 1990 and own data), showing location for samples ALBA-01 to ALBA-31

a deposition age younger than Ordovician for the sedimentary series in Sierra Albarrana according to the deformation, metamorphism and intrusion of granitoids in Early Ordovician times, thus being a record prior to the Ordovician rifting of the Iberian Massif. The fossil content in the Azuaga Formation has provided an Early-Middle Cambrian age to this series (Azor 1994; Liñán 1978; Liñán and Quesada 1990; Jensen et al. 2004). Therefore, an Early Cambrian age can be attributed to the units of the Sierra Albarrana Group from the Azuaga Formation downwards (Azor 1994; Azor and Ballèvre 1997; Jensen et al. 2004).

3 Whole rock geochemistry

3.1 Rock sampling and petrography

Thirty one samples of siliciclastic rocks (3 feldspathic quartzites and 28 meta-sandstones/meta-shales) were collected from the four successions of the Sierra Albarrana Group (Fig. 3). Table 1 shows sample details, including their location, while Fig. 4 illustrates their main petrographic features. The three quartz-feldspathic samples of the Albarrana Succession (ALBA-01 to ALBA-03) are essentially composed of Qz and Pl, with Ms, Bt, and Kfs, and Rt as main accessory (mineral abbreviations after Whitney and Evans 2010) (Fig. 4a). Among the meta-sandstones and meta-shales, eight samples were collected from the Cabril-Peña Grajera Succession (ALBA-04 to ALBA-11). They are fine-grained, grey-greenish, low strained rocks that change to medium-grained textures near quartzite layers (ALBA-09 to ALBA-11). The mineral assemblage observed in these rocks is composed of Qz, Pl, Kfs, Bt, Ms and Sil, with Tur and opaque as main accessory minerals (Fig. 4b, c). Fourteen metasedimentary rocks were collected in the Albariza-Bembézar Succession (ALBA-12 to ALBA-25). They consist of fine to medium-grained phyllites, mica-schists, and metagreywackes which may contain Grt, St, And, Sil, Qz, Pl, Bt, Ms, Chl, with Tur and opaque as the main accessory minerals. They define a metamorphic sequence with rapid decreasing P–T conditions from bottom to top (Fig. 4d–f). Finally, six fine-grained phyllites and metagreywackes were collected in the Azuaga Formation (ALBA-26 to ALBA-31). They present a lepidoblastic fabric with Qz, Pl, Bt, Ms, and Chl as the most frequently observed minerals (Fig. 4g, h).

3.2 Analytical methods

Geochemical and isotope analyses were performed on firstly crushed and powdered rock samples at Universidad Complutense de Madrid (Spain). Major and trace elements were analyzed at Activation Laboratories Ltd. (Actlabs, Canada) following a fusion sample digestion with lithium metaborate or tetraborate, and ICP-OES (for major elements and Sc, Be, V, Zr, Ba, and Sr) and ICP-MS (for the rest of trace elements) analytical procedures. Along with the samples, two sample duplicates, two procedural method blanks, and fourteen international standards materials were analyzed in order to verify the quality of the analyses. The complete list of these certified and measured results are included in Supplementary Quality Control Table. The detection limits for the analytical procedure range from 0.01% for the majority of the major elements to 0.001% for TiO_2 and MnO; and for the trace elements, from 0.002 ppm for the Lu to 30 ppm for the Zn contents. Resulting data for the major and trace elements geochemical analysis are given in Table 2, and in Table 3 for rare earth elements (REE).

Sm–Nd isotope analyses (Table 4) were performed at Geochronological Service of Universidad Complutense de Madrid, using Isotope Dilution Mass Spectrometry (ID-TIMS). Samples were spiked with a mixed ^{149}Sm–^{150}Nd tracer before performing a sample dissolution with ultra-clean reagents (HF-HNO_3-HCl). The resulting solutions were passed through a double step chromatographic separation, by using DOWEX AG®50×8, in order to separate the complete REE group from the bulk matrix of the sample and in a second stage, LnResin® (Eichrom Technologies, Inc., USA) for a complete separation of Sm and Nd. Both purified fractions were loaded, together with 1 µl of ultrapure 0.05 M H_3PO_4, on a pre-cleaned Re triple-filament arrangement and analyzed on an IsotopX-Phoenix® mass spectrometer (TIMS), following a single and a multi-dynamic collection procedure for Sm and Nd analysis, respectively. A normalized value of 0.7219 for the $^{146}Nd/^{144}Nd$ ratio (O'Nions et al. 1979) was considered for a continuous correction of the Nd-isotope fractionation. Likewise, corrections for the presence of ^{142}Ce and ^{144}Sm isotopes were continuously performed to prevent isobaric interferences during the analysis. Seven replicas of the Nd-reference standard JNdi-1 (Tanaka et al. 2000) were run along with the samples, yielding an average value of $^{143}Nd/^{144}Nd = 0.512107$, with an internal precision of ± 0.000005 (2σ). Analytical errors on $^{147}Sm/^{144}Nd$ and $^{143}Nd/^{144}Nd$ ratios were estimated at less than 0.1% and 0.006%, respectively, with a total Sm and Nd procedural method blank under 0.1 ng.

3.3 Results

3.3.1 Geochemical classification

Major and trace elemental concentrations are given in Table 2. When plotting the major elements on the Herron (1988) geochemical classification diagram (Fig. 5a), the majority of the fine and medium-grained schistose samples plot in the shale field, closer to the Post Archean Australian Shale (PAAS; Taylor and MacLennan 1985), some

Table 1 Information of the studied samples (metasedimentary rocks from Sierra Albarrana Group—SW Iberian Massif)

Sample #	Structural position	UTM30 co-ordinates		Lithology
ALBA-01	Albarrana succession	287,464	4,216,474	Fine-grained feldsphatic metaquartzite
ALBA-02	Albarrana succession	287,464	4,216,474	Fine-grained feldsphatic metaquartzite
ALBA-03	Albarrana Succession	287,464	4,216,474	Fine-grained feldsphatic metaquartzite
ALBA-04	Cabril-Peña Grajera succession (N flank of the anticline)	289,309	4,214,524	Paragneiss (fine-grained metagreywacke)
ALBA-05	Cabril-Peña Grajera succession (N flank of the anticline)	289,292	4,214,580	Paragneiss (fine-grained metagreywacke)
ALBA-06	Cabril-Peña Grajera succession (N flank of the anticline)	289,292	4,214,580	Paragneiss (fine-grained metagreywacke)
ALBA-07	Cabril-Peña Grajera succession (N flank of the anticline)	289,292	4,214,580	Paragneiss (fine-grained metagreywacke)
ALBA-08	Cabril-Peña Grajera succession (N flank of the anticline)	289,292	4,214,580	Paragneiss (fine-grained metagreywacke)
ALBA-09	Cabril-Peña Grajera succession (N flank of the anticline)	288,842	4,213,824	Brown schistose greywacke (medium grained)
ALBA-10	Cabril-Peña Grajera succession (S flank of the anticline)	288,711	4,213,735	Brown schistose greywacke (medium grained)
ALBA-11	Cabril-Peña Grajera succession (S flank of the anticline)	288,711	4,213,735	Brown schistose greywacke (medium grained)
ALBA-12	Albariza-Bembézar succession	289,989	4,215,357	Medium-grained garnet and andalucite-bearing micaschist
ALBA-13	Albariza-Bembézar succession	289,943	4,215,379	Medium-grained garnet and andalucite-bearing micaschist
ALBA-14	Albariza-Bembézar succession	289,885	4,215,433	Fine-grained garnet bearing micaschist
ALBA-15	Albariza-Bembézar succession	290,184	4,215,621	Fine-grained garnet bearing micaschist
ALBA-16	Albariza-Bembézar succession	290,299	4,215,442	Fine-grained phyllite
ALBA-17	Albariza-Bembézar succession	291,523	4,216,090	Fine-grained phyllite
ALBA-18	Albariza-Bembézar succession	291,549	4,216,133	Fine-grained phyllite
ALBA-19	Albariza-Bembézar succession	291,680	4,216,306	Fine-grained phyllite
ALBA-20	Albariza-Bembézar succession	291,070	4,217,054	Fine-grained schist (metagreywacke)
ALBA-21	Albariza-Bembézar succession	291,070	4,217,054	Fine-grained schist (metagreywacke)
ALBA-22	Albariza-Bembézar succession	290,886	4,217,853	Fine-grained schist (metagreywacke)
ALBA-23	Albariza-Bembézar succession	290,880	4,217,891	Metagreywacke
ALBA-24	Albariza-Bembézar succession	289,456	4,211,646	Low altered schist (fine grained)
ALBA-25	Albariza-Bembézar succession	289,456	4,211,646	Low altered schist (fine grained)
ALBA-26	Azuaga formation	290,717	4,209,381	Fine-grained phyllite
ALBA-27	Azuaga formation	290,717	4,209,381	Fine-grained phyllite
ALBA-28	Azuaga formation	279,152	4,225,256	Fine-grained phyllite (metagreywacke)
ALBA-29	Azuaga formation	279,184	4,225,259	Metagreywacke
ALBA-30	Azuaga formation	279,163	4,225,054	Metagreywacke
ALBA-31	Azuaga formation	279,163	4,225,054	Metagreywacke

of them closer to the limit with the wacke field, matching stronger sandy features observed in the petrographic study (Table 1), and higher SiO_2/Al_2O_3 ratios (Table 2). Five samples fall within the wacke field (ALBA-04, -06, -07, -23, and -31), which confirms field and petrographic observations. Meanwhile, quartzites samples from the Albarrana Succession (AS) plot in the arkose field, displaying the lowest values for the SiO_2/Al_2O_3 ratios and very low K-contents (Fig. 5b). From the arkosic and relative immature character of the Albarrana quartzites, an increase of the sedimentary maturity can be observed from the Cabril-Peña Grajera Succession (CGS) to the Albariza-Bembézar Succession (ABS) and Azuaga Formation (AzF) samples. Samples from these two latter successions share a similar geochemical composition. AS and CGS samples show higher SiO_2/Al_2O_3 (8.30 and 4.17, respectively) and lower K_2O/Na_2O ratios (0.12 and 1.86, respectively) than those observed in the PAAS (3.32 and 3.08, respectively).

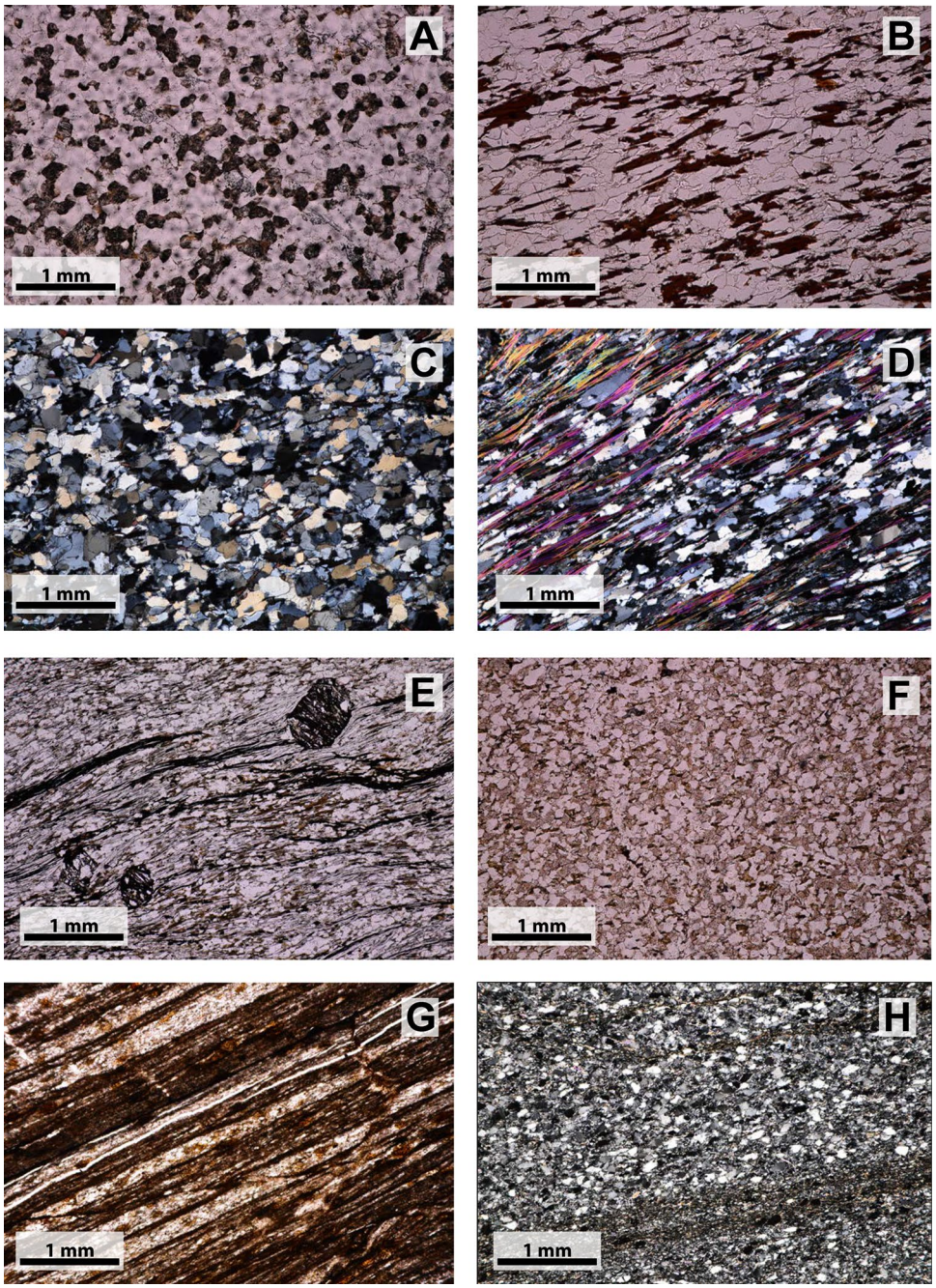

Fig. 4 Petrographic microphotographs showing textural features of the most representative rocks in the Sierra Albarrana Group. **a** Fine-grained feldspathic metaquartzite from Albarrana Succession; **b** Paragneiss from Cabril-Peña Grajera Succession; **c** Fine-grained metagreywacke from Cabril-Peña Grajera Succession; **d** Fine-grained micaschist from Albariza-Bembézar Succession; **e** Fine-grained garnet bearing phyllite from Albariza-Bembézar Succession; **f** Fine-grained metagreywacke from Albariza-Bembézar Succession; **g** Fine-grained phyllite from Azuaga Formation; and **h** Metagreywacke from Azuaga Formation

The latter implies a relative immature character, with a predominance of plagioclase over K-feldspar, compatible with very low values of K_2O in the quartzite samples (avg. 0.37 wt.%) (Fig. 5b). High SiO_2 contents (82.25 wt.% and 63.75 wt.%, avg. values for AS and CGS, respectively) and particularly a relative lower Al_2O_3 abundances (10.14 wt.% and 15.81 wt.%, avg. values for AS and CGS, respectively) are probably related to a limited presence of micas, as confirmed by a negative or very poor correlation between Al, Fe, and K in the samples from these two units. On the contrary, the metasedimentary samples from the ABS and AzF show lower SiO_2 and higher Al_2O_3 abundances (60.10 and 63.91 wt.%, and 20.60 and 18.18 wt.%, respectively), with SiO_2/Al_2O_3 (3.10 and 3.57) and K_2O/Na_2O ratios (2.85 and 2.24) closer to those of the PAAS, indicating a strong pelitic character, in agreement with an increase in sedimentary maturity (Fig. 5a). This is also confirmed by Al_2O_3/TiO_2 (20.85 and 22.89) and Al_2O_3/Na_2O (13.13 and 10.86) ratios within the range of those of the PAAS (18.90 and 15.75, respectively).

Table 2 Whole rock major and trace element data of metasedimentary rocks from SW Iberian Autochthonous Domain (Sierra Albarrana Group)

	ALBA-01	ALBA-02	ALBA-03	ALBA-04	ALBA-05	ALBA-06	ALBA-07	ALBA-08	ALBA-09	ALBA-10	ALBA-11	ALBA-12	ALBA-13	ALBA-14	ALBA-15	ALBA-16	ALBA-17	ALBA-18	ALBA-19	ALBA-20	ALBA-21	ALBA-22	ALBA-23	ALBA-24	ALBA-25	ALBA-26	ALBA-27	ALBA-28	ALBA-29	ALBA-30	ALBA-31
SiO_2	83.03	85.76	77.95	69.16	64.51	72.28	71.14	53.28	58.67	61.37	59.6	59.28	58.32	57.95	59.99	61.02	55.15	53.84	55.9	66.64	66.33	54.19	75.9	57.76	59.11	67.32	61.58	59.58	62.13	63.45	69.38
Al_2O_3	9.49	8.85	12.07	14.85	17.91	12.26	12.98	18.43	18.09	15.54	16.41	20.92	20.34	21.19	20.25	18.49	23.47	25.53	24.76	16.31	15.8	24.55	11.96	23.2	21.67	16.66	19.47	20.23	19.05	18.59	15.06
Fe_2O_3	0.22	0.24	0.16	3.92	4.67	3.9	3.52	7.18	6.73	6.41	7.1	6.44	7.25	7.72	6.76	6.2	6.96	6.58	6.35	6.25	5.98	6.43	3.76	5.34	5.54	4.62	6	7.46	6.15	5.63	5.03
MnO	0.011	0.017	0.01	0.033	0.028	0.016	0.021	0.043	0.047	0.046	0.031	0.031	0.05	0.063	0.055	0.057	0.095	0.089	0.096	0.055	0.102	0.056	0.026	0.128	0.059	0.044	0.063	0.079	0.069	0.071	0.057
MgO	0.07	0.04	0.07	1.45	1.61	1.22	1.16	2.13	1.92	4.09	3.63	1.72	1.29	0.74	1.37	1.56	1.4	1.47	1.43	0.62	0.37	1.39	0.77	1.41	1.29	0.99	1.38	2.34	1.85	1.39	1.18
CaO	2.07	1.79	2.08	2.4	2.93	0.56	1.11	3.76	0.79	1.17	0.68	0.44	0.59	0.5	0.55	1.09	0.35	0.5	0.52	0.21	0.41	0.35	0.32	0.28	0.62	0.62	0.72	0.55	0.73	0.24	0.62
Na_2O	3.01	2.67	3.4	3.12	4.69	1.95	3.01	3.26	1.38	2.7	3.24	1.23	1.13	1.4	1.12	1.92	1.43	1.49	1.38	1.38	3.3	1.66	3.94	1.99	2.58	1.95	1.5	1.23	2.3	2.01	1.56
K_2O	0.26	0.33	0.53	2.45	1.32	5.4	3.67	6.57	5.31	5.07	6.78	5.15	5.03	4.92	5.22	4.05	4.84	5.19	5.07	3.24	2.49	5.55	0.95	4.36	3.86	3.42	4.11	4.26	3.62	3.95	3.02
TiO_2	0.18	0.305	1.385	0.717	0.93	0.47	0.796	0.933	0.959	0.719	0.779	1.098	1.154	1.392	1.1	1.167	1.162	1.196	1.03	0.774	0.714	1.059	0.454	0.977	0.914	0.76	0.877	0.669	0.703	0.982	0.889
P_2O_5	< 0.01	< 0.01	< 0.01	0.17	0.1	0.04	0.05	0.15	0.2	0.17	0.14	0.17	0.16	0.17	0.26	0.22	0.14	0.19	0.15	0.13	0.13	0.1	0.12	0.1	0.12	0.09	0.1	0.13	0.12	0.11	0.46
LOI[a]	0.27	0.38	0.75	1.66	1.65	0.65	0.81	4.22	4.39	1.51	1.03	3.09	3.39	4.6	4.02	3.17	4.71	4.2	3.96	3.83	3.22	4.94	1.86	4.23	4.26	3.64	4.62	4.27	3.53	3.36	2.58
Total	98.61	100.4	98.41	99.93	100.3	98.75	98.26	99.94	98.49	98.79	99.43	99.57	98.72	100.7	100.7	98.96	99.73	100.3	100.7	99.44	98.83	100.3	100.1	99.77	100	100.1	100.4	100.8	100.2	99.79	99.84
Sc	1	< 1	3	12	15	5	8	16	17	15	16	19	18	18	17	16	19	20	18	12	11	20	5	16	15	11	15	18	17	15	15
Be	2	2	4	3	6	1	2	3	4	3	4	4	4	4	4	4	5	5	4	3	5	5	3	4	5	3	4	4	5	4	3
V	14	14	59	68	91	38	51	88	110	103	98	124	125	124	108	107	121	129	119	88	75	116	27	110	97	77	91	115	113	99	79
Cr	< 20	< 20	70	60	80	40	40	90	90	80	80	100	100	100	80	90	100	100	90	70	60	110	30	100	80	60	80	90	90	80	60
Co	3	10	4	22	16	30	15	18	17	18	8	20	20	24	13	16	16	17	13	13	17	12	13	12	10	11	14	18	16	16	9
Ni	< 20	< 20	< 20	20	40	< 20	20	40	50	40	40	50	40	50	40	30	40	40	30	30	30	40	< 20	20	30	< 20	30	50	40	40	< 20
Cu	< 10	< 10	< 10	20	< 10	< 10	< 10	10	20	< 10	< 10	40	30	20	30	30	30	20	30	< 10	40	40	< 10	30	50	30	20	30	20	20	10
Zn	< 30	< 30	< 30	40	40	< 30	< 30	< 30	< 30	< 30	< 30	110	120	110	50	90	100	100	90	< 30	50	< 30	30	70	60	140	70	110	90	80	50
Ga	9	7	9	20	21	19	17	22	28	24	24	33	32	32	29	30	34	36	35	24	19	37	11	33	31	24	26	28	26	27	20
Rb	8	9	18	79	67	191	118	320	245	175	232	207	213	200	182	184	195	218	231	142	133	233	46	178	168	135	173	191	167	180	127
Sr	251	225	260	295	277	165	195	245	124	133	111	115	128	190	82	152	155	182	145	115	198	136	131	184	211	124	138	150	214	183	155
Y	1.6	1.7	6	39.3	48	30	28.6	41.8	42.5	30.2	26.9	45.6	48.2	54.7	54.2	57.8	30.1	37.1	32.4	37.2	45.3	50.1	32.4	25.8	22.5	35.3	36.9	28.9	37.7	34.3	64.5
Zr	103	245	1113	377	325	434	652	248	315	138	123	329	319	533	517	571	196	212	224	265	265	165	378	188	217	332	221	158	169	241	787
Nb	2.7	5.9	19.8	10.7	16.3	8.8	12.9	21	19.2	10.7	13.7	25.2	25.4	28	24.1	23.9	26.7	26	24.1	15.2	13.1	27.5	8.8	22.8	22.8	16.2	17.9	16.6	16.7	21.1	19.3
Cs	0.4	0.5	1.3	3.3	3.4	4.7	2.5	4.9	18.3	10	8.1	7.7	9.5	7.5	5.6	9.8	4.2	3.9	5	5.9	3.8	7	1	5.5	4.3	7.2	5.9	7.1	5.4	7.5	4.8
Ba	47	73	110	1450	244	2168	1219	1239	506	568	815	1072	1092	1035	1245	1087	971	1004	1046	643	439	868	155	876	806	1092	907	859	708	911	610
Hf	3	6.6	31.4	9.8	9	11.3	17	7.3	8.6	3.9	3.8	9.7	9.1	14.9	14.4	16.1	6	6.4	6.7	7.7	7.2	5.3	9.1	5.5	6.4	9.1	6.4	4.3	4.9	7	21.8
Ta	0.36	0.71	2.81	1.31	1.53	1.05	1.72	1.63	1.45	0.91	1.12	1.85	1.94	2.29	1.92	1.95	2.14	2.05	1.79	1.34	1.18	1.89	0.9	1.61	1.66	1.31	1.34	1.16	1.17	1.53	1.65
Pb	< 5	< 5	5	19	15	7	8	< 5	8	5	6	40	31	32	20	35	33	33	32	16	30	< 5	7	25	46	69	19	15	18	19	19
Th	5.57	10.3	13.6	20.7	21.8	18.1	29.4	19.1	19.3	10.8	12.1	27.3	27.4	32	29.6	30.9	21.6	18.6	18.4	13.9	14.1	24.6	16	21.1	16.6	16.8	17.6	17	16.3	17	27.9
U	0.59	1.11	3.27	4.14	4.96	4.43	5.05	3.74	5.28	2.83	3.77	5.89	6.13	6.38	6.42	6.38	4.25	3.28	3.95	3.32	2.94	5.57	3.15	3.84	4.28	3.99	3.99	3.26	3.32	3.1	7.18
SiO_2/Al_2O_3	8.75	9.69	6.46	4.66	3.60	5.90	5.48	2.89	3.24	3.95	3.63	2.83	2.87	2.73	2.96	3.30	2.35	2.11	2.26	4.09	4.20	2.21	6.35	2.49	2.73	4.04	3.16	2.95	3.26	3.41	4.61
K_2O/Na_2O	0.09	0.12	0.16	0.79	0.28	2.77	1.22	2.02	3.85	1.88	2.09	4.19	4.45	3.51	4.66	2.11	3.38	3.48	3.67	2.35	0.75	3.34	0.24	2.19	1.50	1.75	2.74	3.46	1.57	1.97	1.94
Al_2O_3/TiO_2	52.72	29.02	8.71	20.71	19.26	26.09	16.31	19.75	18.86	21.61	21.07	19.05	17.63	15.22	18.41	15.84	20.20	21.35	24.04	21.07	22.13	23.18	26.34	23.75	23.71	21.92	22.20	30.24	27.10	18.93	16.94
Al_2O_3/Na_2O	3.15	3.31	3.55	4.76	3.82	6.29	4.31	5.65	13.11	5.76	5.06	17.01	18.00	15.14	18.08	9.63	16.41	17.13	17.94	11.82	4.79	14.79	3.04	11.66	8.40	8.54	12.98	16.45	8.28	9.25	9.65

Table 2 (continued)

	ALBA-01	ALBA-02	ALBA-03	ALBA-04	ALBA-05	ALBA-06	ALBA-07	ALBA-08	ALBA-09	ALBA-10	ALBA-11	ALBA-12	ALBA-13	ALBA-14	ALBA-15	ALBA-16	ALBA-17	ALBA-18	ALBA-19	ALBA-20	ALBA-21	ALBA-22	ALBA-23	ALBA-24	ALBA-25	ALBA-26	ALBA-27	ALBA-28	ALBA-29	ALBA-30	ALBA-31
Rb/Sr	0.03	0.04	0.07	0.27	0.24	1.16	0.61	1.31	1.98	1.32	2.09	1.80	1.66	1.05	2.22	1.21	1.26	1.20	1.59	1.23	0.67	1.71	0.35	0.97	0.80	1.09	1.25	1.27	0.78	0.98	0.82
Cr/Th			5.15	2.90	3.67	2.21	1.36	4.71	4.66	7.41	6.61	3.66	3.65	3.13	2.70	2.91	4.63	5.38	4.89	5.04	4.26	4.47	1.88	4.74	4.82	3.57	4.55	5.29	5.52	4.71	2.15
Cr/V			1.19	0.88	0.88	1.05	0.78	1.02	0.82	0.78	0.82	0.81	0.80	0.81	0.74	0.84	0.83	0.78	0.76	0.80	0.80	0.95	1.11	0.91	0.82	0.78	0.88	0.78	0.80	0.81	0.76
Y/Ni				1.97	1.20		1.43	1.05	0.85	0.76	0.67	0.91	1.21	1.09	1.36	1.93	0.75	0.93	1.08	1.24	1.51	1.25		1.29	0.75		1.23	0.58	0.94	0.86	
Sc/Th	0.18		0.22	0.58	0.69	0.28	0.27	0.84	0.88	1.39	1.32	0.70	0.66	0.56	0.57	0.52	0.88	1.08	0.98	0.86	0.78	0.81	0.31	0.76	0.90	0.65	0.85	1.06	1.04	0.88	0.54
Th/Sc	5.57		4.53	1.73	1.45	3.62	3.68	1.19	1.14	0.72	0.76	1.44	1.52	1.78	1.74	1.93	1.14	0.93	1.02	1.16	1.28	1.23	3.20	1.32	1.11	1.53	1.17	0.94	0.96	1.13	1.86
La/Sc	1.28		0.67	5.64	4.80	3.52	16.50	4.18	4.19	2.80	2.75	4.67	5.02	4.58	4.95	5.64	4.37	2.99	3.32	4.72	4.39	4.78	6.48	5.03	3.57	3.67	2.07	2.41	3.05	3.21	4.25
Co/Th	0.54	0.97	0.29	1.06	0.73	1.66	0.51	0.94	0.88	1.67	0.66	0.73	0.73	0.75	0.44	0.52	0.74	0.91	0.71	0.94	1.21	0.49	0.81	0.57	0.60	0.65	0.80	1.06	0.98	0.94	0.32
Nb/Y	1.69	3.47	3.30	0.27	0.34	0.29	0.45	0.50	0.45	0.35	0.51	0.55	0.53	0.51	0.44	0.41	0.89	0.70	0.74	0.41	0.29	0.55	0.27	0.88	1.01	0.46	0.49	0.57	0.44	0.62	0.30
Zr/Ti	0.10	0.13	0.13	0.09	0.06	0.15	0.14	0.04	0.05	0.03	0.03	0.05	0.05	0.06	0.08	0.08	0.03	0.03	0.04	0.06	0.06	0.03	0.14	0.03	0.04	0.07	0.04	0.04	0.04	0.04	0.15
Th/U	9.44	9.28	4.16	5.00	4.40	4.09	5.82	5.11	3.66	3.82	3.21	4.63	4.47	5.02	4.61	4.84	5.08	5.67	4.66	4.19	4.80	4.42	5.08	5.49	3.88	4.21	4.41	5.21	4.91	5.48	3.89
La/Th	0.23	0.09	0.15	3.27	3.30	0.97	4.49	3.50	3.69	3.89	3.64	3.25	3.30	2.58	2.84	2.92	3.84	3.22	3.25	4.07	3.43	3.88	2.03	3.82	3.23	2.40	1.76	2.55	3.18	2.84	2.28
Zr/Sc	103.00		371.00	31.42	21.67	86.80	81.50	15.50	18.53	9.20	7.69	17.32	17.72	29.61	30.41	35.69	10.32	10.60	12.44	22.08	24.09	8.25	75.60	11.75	14.47	30.18	14.73	8.78	9.94	16.07	52.47
CIA[b]	51	53	55	56	56	55	55	49	67	57	55	72	72	72	72	67	75	75	75	74	65	73	61	74	70	68	71	73	69	71	72
PIA[c]	51	53	55	57	56	61	57	49	79	62	59	86	85	85	87	75	87	87	87	85	69	86	62	84	77	76	81	85	76	80	82
ICV[d]	0.6	0.6	0.6	0.9	0.9	1.1	1.0	1.3	0.9	1.3	1.4	0.8	0.8	0.8	0.8	0.9	0.7	0.6	0.6	0.8	0.8	0.7	0.9	0.6	0.7	0.7	0.8	0.8	0.8	0.8	0.8

Oxides are in weight percent (wt.%). Trace elements are in parts per million (ppm)

[a]Loss on ignition

[b]CIA (Chemical Index of Alteration; Nesbitt and Young 1982)

[c]PIA (Plagioclase Index of Alteration; Fedo et al. 1995)

[d]ICV (Index of Compositional Variability; Cox et al. 1995)

Table 3 Whole rock rare earth element data of metasedimentary rocks from SW Iberian Autochthonous Domain (Sierra Albarrana Group)

	ALBA-01	ALBA-02	ALBA-03	ALBA-04	ALBA-05	ALBA-06	ALBA-07	ALBA-08	ALBA-09	ALBA-10	ALBA-11	ALBA-12	ALBA-13	ALBA-14	ALBA-15	ALBA-16	ALBA-17	ALBA-18	ALBA-19	ALBA-20	ALBA-21	ALBA-22	ALBA-23	ALBA-24	ALBA-25	ALBA-26	ALBA-27	ALBA-28	ALBA-29	ALBA-30	ALBA-31
La	1.28	0.92	2	67.7	72	17.6	132	66.8	71.2	42	44	88.7	90.3	82.4	84.2	90.2	83	59.8	59.8	56.6	48.3	95.5	32.4	80.5	53.6	40.4	31	43.4	51.8	48.2	63.7
Ce	2.56	1.69	4.23	145	145	36	263	128	132	81	85.1	175	182	186	171	189	149	133	112	111	106	182	66	152	101	82.8	82	83.9	97.9	107	140
Pr	0.25	0.17	0.41	14.6	15.2	3.66	27.4	13.9	14.9	9.16	9.05	19.1	19.7	18	18.2	20.1	17.3	12.9	12.9	12.6	12	19.9	7.15	16.5	11.3	9.66	7.7	9.42	11.4	10.8	14.6
Nd	0.97	0.64	1.56	54.8	57.1	14	102	52.4	54.9	34.1	33.6	71.4	74.5	67.9	69.1	77.3	64.3	48.8	48.3	50.6	49.1	75.4	26.6	62.7	43	37	30.1	36.4	43.8	42.1	57.5
Sm	0.21	0.16	0.35	11.1	11	2.71	18.4	9.68	9.87	6.8	6.19	13.2	14	12.7	13	14.5	11.9	9.1	9.36	9.46	9.75	13.9	4.92	11.3	7.92	7	6.39	6.91	8.22	7.99	11.6
Eu	0.297	0.283	0.371	1.61	1.81	0.554	1.35	1.55	1.93	1.54	1.58	2.2	2.41	2.32	2.35	2.36	2.3	2.08	1.72	1.92	2.1	2.56	1.45	2.09	1.83	1.4	1.35	1.45	1.79	1.69	2.34
Gd	0.18	0.15	0.37	9.07	9.38	3.29	12.7	7.82	8.38	5.71	5.18	10.6	11.1	10.9	11.1	12.8	9.62	8.01	7.22	7.85	8.55	11.1	4.99	8.47	6.52	5.82	6.08	5.86	7.34	6.73	10.9
Tb	0.03	0.03	0.07	1.3	1.41	0.64	1.52	1.16	1.24	0.91	0.82	1.51	1.64	1.63	1.64	1.87	1.27	1.17	1.09	1.18	1.34	1.61	0.87	1.09	0.88	0.91	0.95	0.88	1.11	0.98	1.71
Dy	0.22	0.26	0.65	7.14	8.54	4.65	6.68	6.7	7.24	5.37	4.76	8.5	9.02	9.74	9.58	10.4	6.34	6.77	6.11	6.72	7.73	8.77	5.22	5.57	4.63	5.65	6.23	5.43	6.75	5.96	10.6
Ho	0.05	0.05	0.19	1.4	1.68	1.04	1.07	1.35	1.46	1.04	0.93	1.49	1.62	1.86	1.89	1.95	1.04	1.28	1.16	1.26	1.53	1.66	1.15	0.9	0.78	1.17	1.21	1.05	1.32	1.18	2.21
Er	0.16	0.22	0.82	4.05	4.74	3.22	2.9	3.95	4.02	3	2.75	4.23	4.42	5.27	5.66	5.33	2.67	3.55	3.2	3.57	4.29	4.44	3.44	2.36	2.11	3.53	3.44	2.96	3.57	3.26	6.49
Tm	0.033	0.039	0.174	0.571	0.707	0.481	0.385	0.566	0.58	0.461	0.381	0.56	0.629	0.775	0.821	0.75	0.377	0.48	0.467	0.516	0.613	0.607	0.517	0.303	0.269	0.495	0.482	0.447	0.527	0.484	0.944
Yb	0.24	0.38	1.68	3.93	4.57	3.23	2.86	3.97	3.94	2.99	2.65	3.77	3.96	5.1	5.53	5.04	2.42	3.23	2.96	3.39	4.1	4.04	3.34	1.96	1.67	3.31	3.08	2.81	3.51	3.42	6.66
Lu	0.046	0.075	0.363	0.637	0.711	0.507	0.455	0.627	0.603	0.431	0.405	0.582	0.596	0.761	0.881	0.757	0.376	0.475	0.441	0.519	0.623	0.596	0.463	0.312	0.289	0.506	0.476	0.428	0.542	0.485	1.05
ΣREE	7	5	13	323	334	92	573	298	312	195	197	401	416	405	395	432	352	291	267	267	256	422	159	346	236	200	180	201	240	240	330
Eu/Eu*	4.70	5.62	3.17	0.49	0.55	0.57	0.27	0.55	0.65	0.76	0.86	0.57	0.59	0.61	0.60	0.53	0.66	0.75	0.64	0.68	0.71	0.63	0.90	0.66	0.78	0.67	0.67	0.70	0.71	0.71	0.64
$(La/Sm)_N$	3.76	3.55	3.53	3.76	4.04	4.01	4.43	4.26	4.45	3.81	4.39	4.15	3.98	4.00	4.00	3.84	4.30	4.05	3.94	3.69	3.06	4.24	4.06	4.40	4.18	3.56	2.99	3.88	3.89	3.72	3.39
$(Gd/Yb)_N$	0.60	0.31	0.18	1.84	1.64	0.81	3.54	1.57	1.70	1.52	1.56	2.24	2.23	1.70	1.60	2.02	3.17	1.98	1.94	1.85	1.66	2.19	1.19	3.44	3.11	1.40	1.57	1.66	1.67	1.57	1.30
$(La/Yb)_N$	3.57	1.62	0.80	11.52	10.54	3.64	30.86	11.25	12.08	9.39	11.10	15.73	15.25	10.80	10.18	11.97	22.93	12.38	13.51	11.16	7.88	15.81	6.49	27.46	21.46	8.16	6.73	10.33	9.87	9.42	6.40
Ce/Ce*	1.13	1.07	1.17	1.16	1.10	1.12	1.10	1.05	1.02	1.04	1.07	1.07	1.08	1.21	1.10	1.11	0.99	1.20	1.01	1.04	1.10	1.05	1.09	1.05	1.03	1.05	1.33	1.04	1.01	1.18	1.15

Rare earth elements data in parts per million (ppm)

$Eu/Eu^* = Eu_N/\sqrt{(Sm_N \times Gd_N)}$

$Ce/Ce^* = Ce_N/\sqrt{(Sm_N \times Gd_N)}$

Table 4 Whole rock Nd isotope data of metasedimentary rocks from SW Iberian Autochthonous Domain (Sierra Albarrana Group)

Sample	Sm	Nd	$^{147}Sm/^{144}Nd$	$^{143}Nd/^{144}Nd$	± StdErr[b] 10^{-6}	εNd (0)	εNd (530)[b]	TDM (Ma)[a]	$f^{Sm/Nd}$	$^{143}Nd/^{144}Nd$ initial
ALBA-01	0.17	0.85	0.1220	0.511979	2	− 12.9	− 7.8	1766	− 0.3800	0.511555
ALBA-02	0.13	0.60	0.1287	0.512018	6	− 12.1	− 7.5	1837	− 0.3457	0.511571
ALBA-03	0.25	1.33	0.1155	0.511981	7	− 12.8	− 7.3	1646	− 0.4128	0.511580
ALBA-04	9.36	47.88	0.1182	0.511889	2	− 14.6	− 9.3	1840	− 0.3992	0.511478
ALBA-05	11.49	61.31	0.1133	0.511895	1	− 14.5	− 8.9	1741	− 0.4240	0.511501
ALBA-06	2.94	15.38	0.1153	0.511864	2	− 15.1	− 9.6	1825	− 0.4137	0.511464
ALBA-07	15.41	84.20	0.1106	0.511760	2	− 17.1	− 11.3	1897	− 0.4376	0.511376
ALBA-08	8.13	44.15	0.1113	0.512024	2	− 12.0	− 6.2	1515	− 0.4341	0.511638
ALBA-09	8.66	47.44	0.1104	0.511942	1	− 13.6	− 7.7	1623	− 0.4388	0.511558
ALBA-10	5.93	31.15	0.1150	0.511872	2	− 14.9	− 9.4	1807	− 0.4154	0.511473
ALBA-11	5.50	29.92	0.1112	0.512108	2	− 10.3	− 4.5	1388	− 0.4349	0.511722
ALBA-12	11.45	61.60	0.1123	0.511951	1	− 13.4	− 7.7	1639	− 0.4290	0.511561
ALBA-13	13.42	71.19	0.1139	0.511945	2	− 13.5	− 7.9	1675	− 0.4208	0.511550
ALBA-14	10.54	55.68	0.1144	0.511936	1	− 13.7	− 8.1	1697	− 0.4183	0.511539
ALBA-15	11.44	63.05	0.1097	0.511941	2	− 13.6	− 7.7	1613	− 0.4423	0.511560
ALBA-16	12.44	64.55	0.1165	0.511991	2	− 12.6	− 7.2	1646	− 0.4078	0.511587
ALBA-17	9.58	51.99	0.1114	0.511954	1	− 13.3	− 7.6	1620	− 0.4336	0.511567
ALBA-18	8.24	43.73	0.1138	0.511913	1	− 14.1	− 8.5	1723	− 0.4213	0.511518
ALBA-19	7.88	41.96	0.1135	0.511854	1	− 15.3	− 9.7	1806	− 0.4232	0.511460
ALBA-20	9.16	48.08	0.1152	0.511881	2	− 14.8	− 9.3	1796	− 0.4144	0.511481
ALBA-21	8.17	40.47	0.1220	0.511937	1	− 13.7	− 8.6	1837	− 0.3799	0.511513
ALBA-22	11.56	64.00	0.1092	0.511895	2	− 14.5	− 8.6	1673	− 0.4447	0.511516
ALBA-23	5.12	26.07	0.1188	0.511916	2	− 14.1	− 8.8	1808	− 0.3961	0.511504
ALBA-24	11.08	60.19	0.1113	0.511854	1	− 15.3	− 9.5	1769	− 0.4342	0.511467
ALBA-25	7.06	37.27	0.1144	0.511849	2	− 15.4	− 9.8	1832	− 0.4184	0.511452
ALBA-26	6.27	32.70	0.1159	0.511996	2	− 12.5	− 7.1	1629	− 0.4109	0.511593
ALBA-27	5.28	27.39	0.1166	0.511943	2	− 13.6	− 8.1	1724	− 0.4074	0.511538
ALBA-28	6.38	33.19	0.1163	0.511971	2	− 13.0	− 7.6	1676	− 0.4088	0.511567
ALBA-29	7.57	38.95	0.1175	0.511988	1	− 12.7	− 7.3	1669	− 0.4029	0.511580
ALBA-30	7.32	37.85	0.1169	0.511894	1	− 14.5	− 9.1	1807	− 0.4058	0.511489
ALBA-31	10.28	50.99	0.1219	0.511942	1	− 13.6	− 8.5	1827	− 0.3803	0.511519

Decay constant for ^{147}Sm: $6.54 \times 10–12$ $year^{-1}$ (Lugmair and Marti 1978). Present-day CHUR parameters: $^{147}Sm/^{144}Nd = 0.1967$; $^{143}Nd/^{144}Nd = 0.512638$ (Jacobsen and Wasserburg 1980)

[a]Nd model ages calculated according to DePaolo (1981)

[b]εNd(t) calculated for 530 Ma

3.3.2 Source area weathering and recycling

The average CIA (Chemical Index of Alteration; Nesbitt and Young 1982) and PIA (Plagioclase Index of Alteration; Fedo et al. 1995) values for the metasedimentary rocks from Albarrana Succession (53 and 53, respectively) and Cabril-Peña Grajera Succession (56 and 60, respectively) indicate relative fresh rocks and low weathering alteration (Table 2) (Fig. 5b). Both indexes are far below those of the PAAS (CIA = 70; PIA = 79), and imply a limited secondary conversion of plagioclase/K-feldspars to clay minerals. Significant K-addition can be excluded in view of the slightly higher K_2O contents in the CGS metasedimentary samples (avg. 4.57 wt.%) compared to those of the PAAS (3.7 wt.%), and the very low K_2O contents of the quartzites from AS (avg. 0.37 wt.%) (Fig. 5b). As expected, this very low K abundance is in agreement with low contents in other LILE elements (Ba, Rb, and Cs). Low Rb (avg. 11.7 ppm) together with high Sr contents (avg. 245.3 ppm) in these samples provide very low Rb/Sr ratios (0.05), representing a low redistribution of the Sr^{2+} and Ca^{2+}, considering also the high CaO abundances (avg. 1.98 wt.%), and typical Sr abundances for quartz-feldspathic rocks (Mielke 1979). However, the slightly high CaO contents suggest that hydrothermal alteration

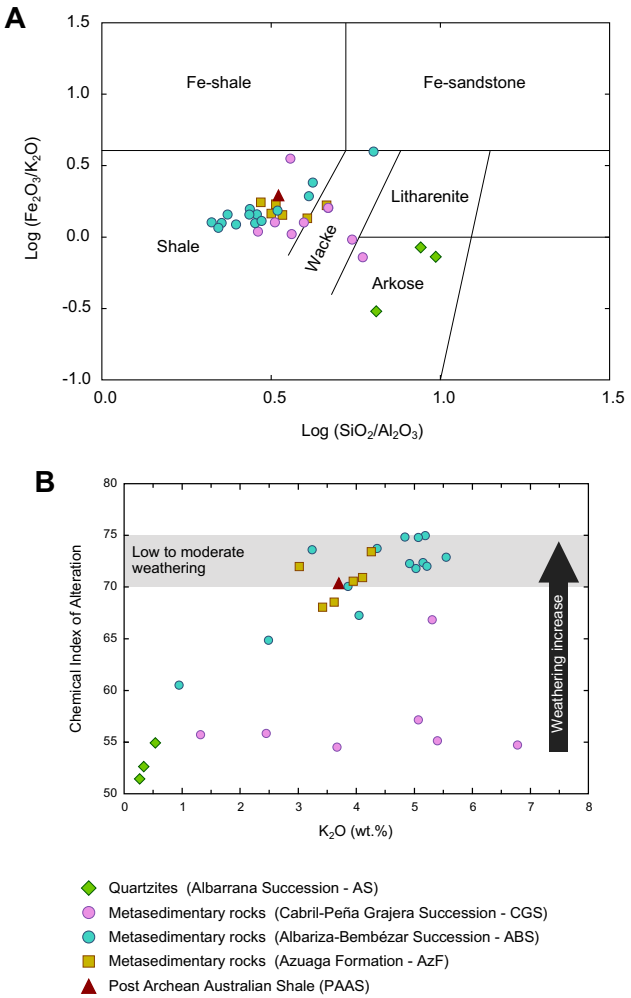

Fig. 5 **a** Chemical classification diagram for siliciclastic sediments (Herron 1988). **b** K_2O vs. Chemical Index of Alteration (CIA; after Nesbitt and Young 1982) for comparison of the source area weathering and recycling in Sierra Albarrana metasedimentary rocks. Post Archean Australian Shale (PAAS; Taylor and McLennan 1985) has been included for comparison

and CaO gain could be ruled out after considering the low LOI values (0.47 and 1.99 for AS and CGS, respectively).

An increase in the chemical maturity is consistent with a higher influence of post-depositional processes over the terrigenous sediments, as confirmed by PIA values for Albariza-Bembézar Succession and Azuaga Formation samples (82 and 80, respectively) (Table 2), which are similar to PAAS (79). This implies certain transformation of plagioclase/feldspar to clay minerals, in agreement with high Al (20.60 and 18.18 wt.%, respectively), and low Ca contents (0.48 and 0.58 wt.% CaO, respectively). Values below 1 of the Index of Compositional Variability (ICV; Cox et al. 1995) calculated for the samples from ABS and AzF (0.7 and 0.8, respectively) imply the presence of clay minerals dominantly with a recycling character.

The relative weathering and post-sedimentary alteration of these samples are confirmed by average CIA values of 71 for both units, matching those of the PAAS (70) and indicating a moderate weathering (Fig. 5b), as also deduced from high Rb/Sr ratios (1.27 and 1.03, respectively), well beyond the 0.5 value that McLennan et al. (1993) suggest for a limited chemical alteration.

3.3.3 Rare earth elements composition (REE)

Quartz-feldspathic Albarrana Succession samples show very low bulk REE contents (avg. 8.3; Table 3), as expected from their high quartz contents, the relative lack of REE-bearing heavy minerals, and the aforementioned small fraction of clay minerals (Taylor and McLennan 1988). Their chondrite-normalized REE patterns (Nakamura 1974; Fig. 6a) are highly influenced by the significant abundance in plagioclase and feldspar (Taylor and McLennan 1988; Condie et al. 1995), where the most distinctive features are a depletion in LREE, a positive trend in HREE ($Gd_N/Yb_N = 0.4$), and a highly positive Eu-anomaly (avg. 4.49), compatible with their high plagioclase fraction and CaO abundances. Sample ALBA-03 presents higher HREE contents, which combined with a very high Zr (1113 ppm) and Hf (31.4 ppm) abundances (Fig. 6c), suggest a likely greater presence of zircon and rutile with low fractionation of the TiO_2, probably accumulated in the coarser fraction of the sediment, since these heavy minerals commonly remain inert through sorting processes (Garcia et al. 1991). By contrast, the bulk REE-abundances in the metasedimentary samples Cabril-Peña Grajera Succession (290.5), Albariza-Bembézar Succession (331.7), and Azuaga Formation (231.9) (Table 3) are above those of the PAAS (184.8), although their chondrite normalized REE patterns are similar (Fig. 6a, b), sharing typical features with felsic igneous sources with an upper crust provenance: (i) a significant LREE fractionation over their HREE abundances, with high La_N/Yb_N ratios (avg. 12.5, 14.5, and 8.5, respectively), (ii) a negative Eu anomaly (0.59, 0.67, and 0.68, respectively) comparable with that of the PAAS (0.65), and finally (iii) almost flat HREE patterns, with Gd_N/Yb_N values close to unity (1.8, 2.2, and 1.5, respectively), and slightly higher than those of the PAAS (1.3). The large variation in LREE for CGS samples (ranging from 74 to 542) (Fig. 6a) is probably because of variable LREE-bearing mineral content (e.g. monazite), as indicated by the wide range in Gd_N/Yb_N ratios (from 0.8 to 3.5) (McLennan 1989; McLennan and Taylor 1991), with an average value typical for igneous rocks with an upper crust affinity. While HREE contents in ABS are controlled by the garnet fraction, zircon is a major factor in HREE abundances for AzF

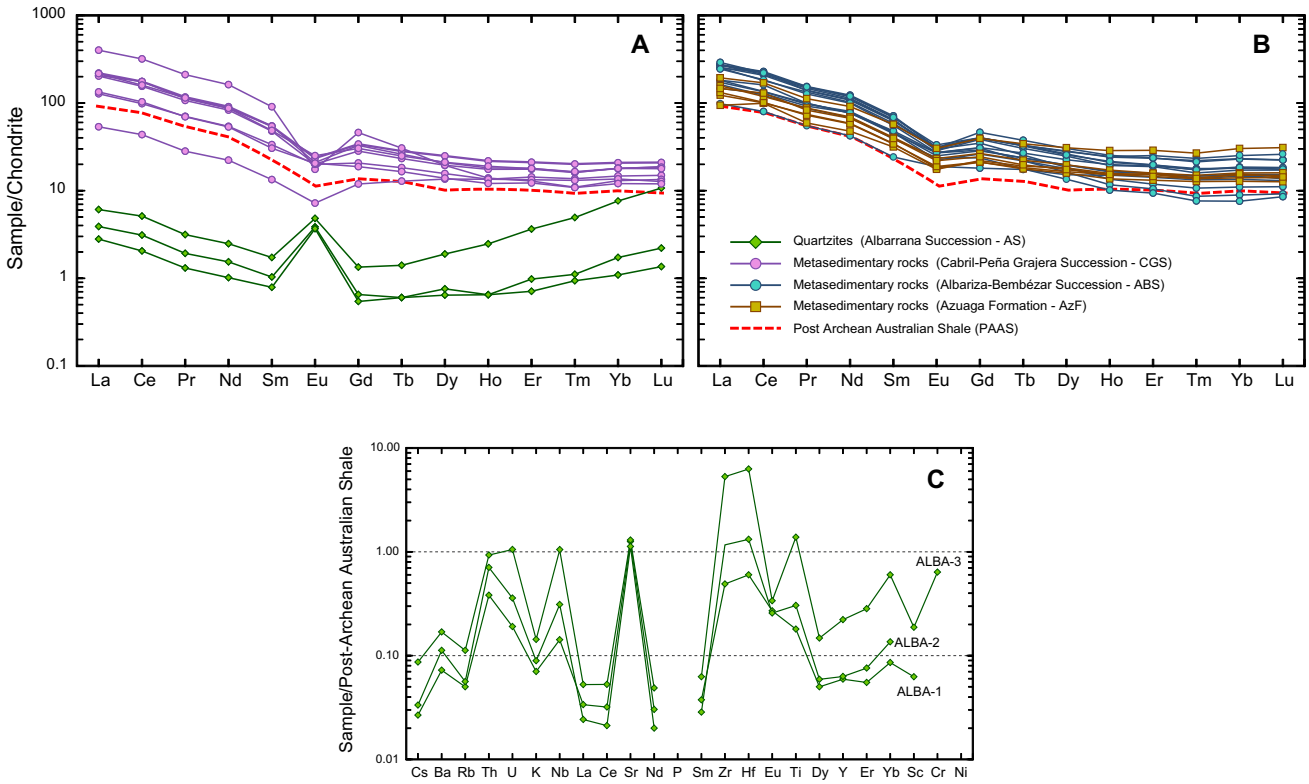

Fig. 6 Chondrite normalized rare earth element plots: **a** Metasedimentary rocks from Albarrana (AS) and Cabril-Peña Grajera (CGS) successions (Samples ALBA-01 to ALBA-11); **b** Metasedimentary rocks from Albariza-Bembézar Succession (ABS) and Azuaga Formation (AzF) (samples ALBA-12 to ALBA-31). Normalizing values are from Nakamura (1974). The dotted line corresponds to the PAAS (Post Archean Australian Shale; Taylor and McLennan 1985). **c** PAAS-normalized trace elements multi-variation diagrams of the Early Cambrian quartzites from Albarrana Succession (AS—Sierra Albarrana Group)

samples, in agreement with a positive correlation between Zr, Hf and HREE contents.

3.3.4 Provenance

In addition to the above mentioned characteristic REE-patterns similar to the PAAS and typical in felsic igneous sources with an upper continental crust affinity, numerous elemental abundances and their ratios suggest dominant felsic contributions for the metasedimentary rocks of the Sierra Albarrana Group. The Al_2O_3/TiO_2 ratios (on average for Albarrana, Cabril-Peña Grajera, Albariza-Bembezar Successions and Azuaga Formation: 30.2, 20.5, 20.9, 22.9, respectively; Table 2) of these two insoluble elements and usually unaffected by weathering processes show values above those of the PAAS (18.9), and support the felsic nature of source rocks. Low Cr and Ni contents are even below the detection limits in the Albarrana Succession quartz-feldspathic samples, and rule out mafic/ultramafic contributions (Armstrong-Altrin et al. 2004). Very low Cr/V ratios (0.88, 0.84, and 0.80 for Cabril-Peña Grajera, Albariza-Bembezar Successions and Azuaga Formation, respectively) (Table 2) and similar to those of the PAAS (0.79) exclude a mafic/ultramafic source, confirmed by high Y/Ni values, displaying a trend to granitic end-members compositions, with an absence of mafic/ultramafic detritus (Hiscott 1984; McLennan et al. 1993) (Fig. 7a). Relatively high La (avg. 64.2, 71.8, and 46.4 ppm, respectively) and Th (avg. 18.9, 22.3, and 18.8 ppm, respectively) abundances found in CGS, ABS, and AzF samples, compared to those of the PAAS (38.0 and 14.6 ppm, respectively) are in agreement with a felsic affinity. Therefore, the comparison between these two latter immobile elements with those commonly associated with mafic/ultramafic source rocks (Sc, Cr and Co), yields very low Sc/Th (avg. 0.78, 0.74, and 0.84 for CGS, ABS, and AzF, respectively) and Cr/Th (avg. 4.19, 4.01, and 4.30, respectively) ratios, lower than those of the PAAS (1.10, and 7.53, respectively), and within the range of felsic rocks (Cox et al. 1995; Cullers, 2002; McLennan et al. 2006) (Fig. 7b). Likewise Cr/Th and Eu/Eu* values (Tables 2, 3) fit those proposed by Cullers (1994) (2.5–17.5 and 0.48–0.78, respectively) for sediments sourced from felsic rocks. The La/Sc vs. Co/Th diagram

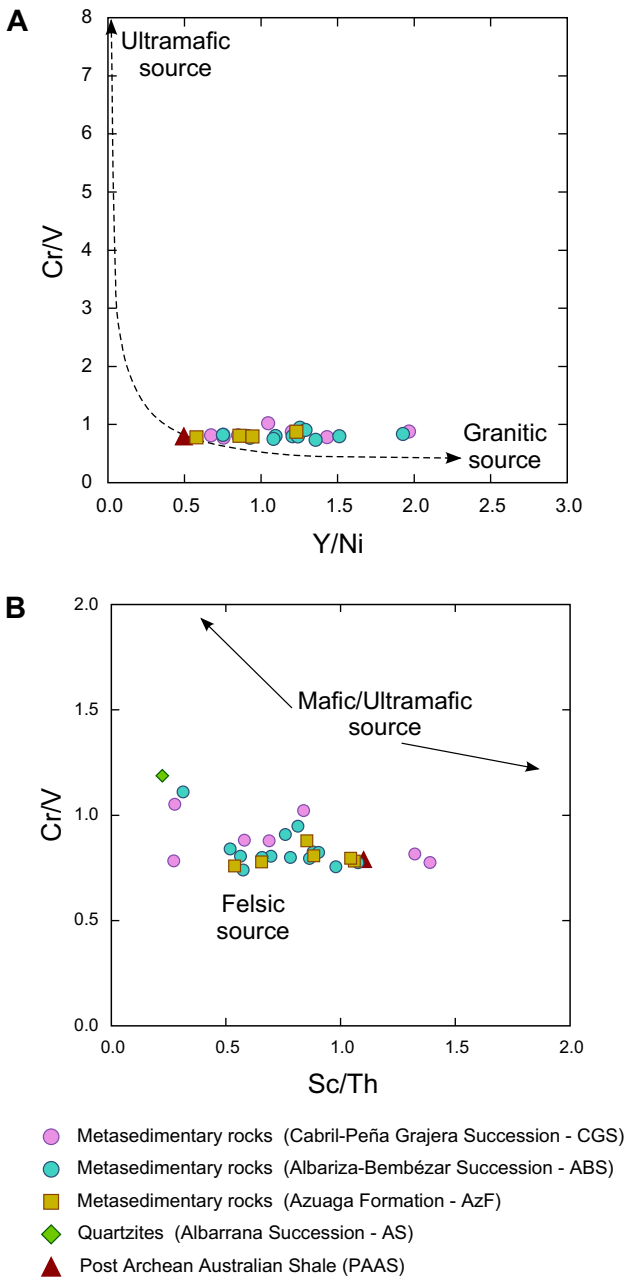

Fig. 7 Provenance discrimination diagrams. **a** Cr/V vs. Y/Ni diagram. The curved line represents the model mixing between ultramafic and granitic end-members (after Hiscott 1984; McLennan et al. 1993). **b** Cr/V vs. Sc/Th showing the affinity of the metasedimentary rocks from Sierra Albarrana Group for a felsic source

(Fig. 8a) places the Sierra Albarrana metasedimentary rocks close to the PAAS and to typical values for felsic volcanic rocks, and far from the common Co/Th and La/Sc values in basaltic and andesitic sources. Felsic volcanic rocks represent an important terrigenous contribution in post-Archean continental arc systems (Condie et al. 1993). In differentiating specific felsic volcanic compositions, the Nb/Y vs Zr/Ti diagram in Fig. 8b shows that most of the samples plot in the rhyodacite/dacite composition field, following the Rhyolitic/dacitic trend (Winchester and Floyd 1977; Fralick and Kronberg 1997).

3.3.5 Tectonic setting

A set of PAAS-normalised major and trace elements diagrams from three units described in Sierra Albarrana Group are presented in Fig. 9, with the exception of the three quartz-feldspathic samples from the Albarrana Succession, whose abundances represent an almost widespread compositional depletion related to PAAS (Fig. 6c). The patterns displayed by the three units match those proposed by Winchester and Max (1989) for passive continental margins (Fig. 9), and also match those found in Early Cambrian shales (slates) from the autochthonous section in the southern Central Iberian Zone (Pusa Gp; Fuenlabrada et al. 2016) and in Middle Cambrian metapelitic rocks from the NW Basal Allochthonous Units (Fuenlabrada et al. 2012). Both are indicative of an upper continental crust provenance, whose sedimentation was influenced by the earlier stages of a Cambrian–Ordovician passive margin (Pieren Pidal 2000; Díez Fernández et al. 2010; Fuenlabrada et al. 2020). They show an average geochemical composition similar to PAAS, with the majority of the normalized major and trace elements close to unity, with no evident depletion in LILE elements, and negative anomalies in different proportions in the case of Sr, P, and Ti abundances (Fig. 9). They all suggest an important influence of the sedimentary processes over the terrigenous sediments, as a result of distant source areas and effective recycling processes. This is confirmed by Th/U ratios (avg. 7.6, 4.4, 4.8, and 4.7 for AS, CGU, ABU, and AzU, respectively) around those of PAAS (4.7), and above typical values for sedimentary rocks sourced from crustal igneous rocks with cratonic provenance (3.5–4.0; McLennan et al. 1993).

The geochemistry of the metasedimentary rocks from Sierra Albarrana Group is compatible with deposition in a peri-continental section influenced by a continental active margin that evolved to a more stable environment (passive margin?) during Early Cambrian times. The La/Th versus Hf diagram (Fig. 10a) shows some affinity for acidic arc sources, some samples having similar values to those of the PAAS (average value for upper continental crust). However, the majority of the samples displays an evident trend to higher Hf contents, which according to Floyd and Leveridge (1987) could be consequence of the erosion effect of a continental basement with increasingly older metasedimentary rocks. Such trend in the denudation process could explain the increase in maturity observed in the Sierra Albarrana Group, with a progressive release of zircon and other accessory, but highly stable minerals and the subsequent enrichment in Zr and Hf that is typical for passive margin sediments (Bhatia and Crook 1986;

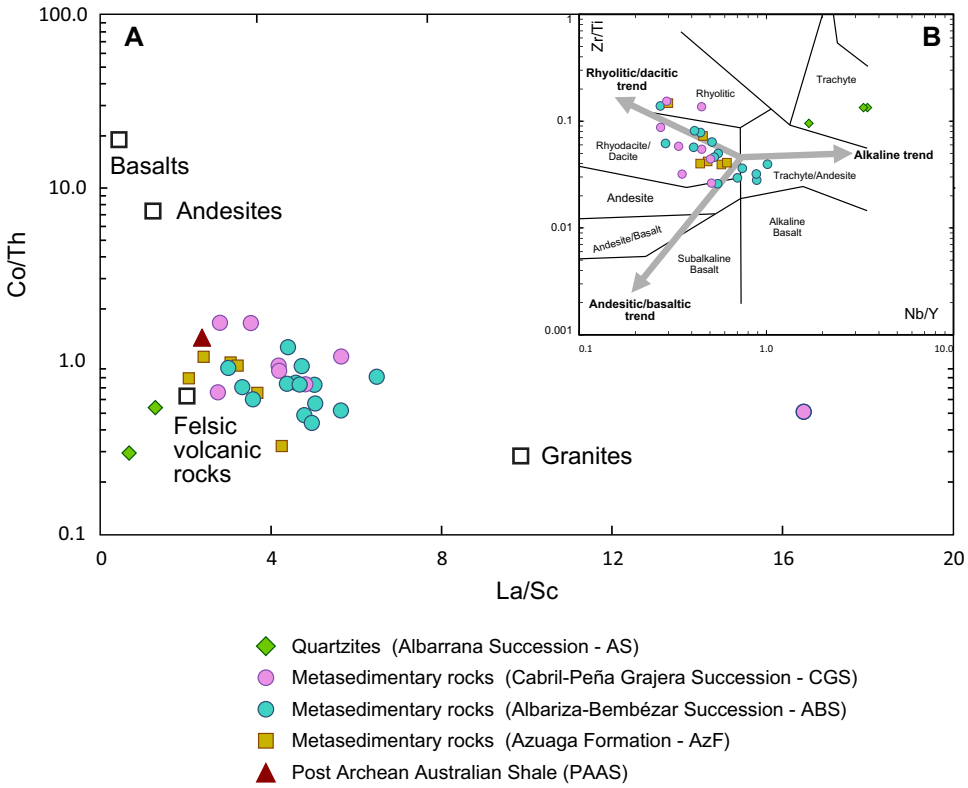

Fig. 8 **a** Co/Th vs. La/Sc diagram for provenance discrimination of siliciclastic rocks (average compositions of igneous rocks from Condie 1993). **b** Zr/Ti vs. Nb/Y diagram (fields after Winchester and Floyd 1977; Fralick and Kronberg 1997) showing affinity for felsic volcanic rhyolitic/dacitic sources

McLennan et al. 1993). Supporting the latter idea, the Th/Sc and Zr/Sc ratios (Table 2) (Fig. 10b) show values that suggest sorting and recycling to some extent, what fits with passive margin turbidites better than with sediments related to an active arc, which would follow normal geochemical compositional variations and limited recycling (McLennan et al. 1993; Cox et al. 1995) (Fig. 10b).

3.3.6 Sm–Nd isotopes

The Sm–Nd isotope data for the Sierra Albarrana metasedimentary rocks are given in Table 4 and Fig. 11. An Early Cambrian maximum depositional age (ca. 530 Ma) has been selected for $\varepsilon Nd_{(i)}$ calculations. No significant variation is observed in the whole group of samples, which defines a single Nd-isotope population. Relatively similar $^{143}Nd/^{144}Nd$ initial ratios, ranging from 0.51138 to 0.51172, suggest a likely common source for all of them. Their $^{147}Sm/^{144}Nd$ ratios (from 0.1092 to 0.1287) are similar to those of continental crust (~0.12; DePaolo 1983), and always below the limit ($^{147}Sm/^{144}Nd = 0.165$), defined by Stern (2002) for reliable Nd model age calculations, sharing typical values among clastic sediments (0.1–0.13; Zhao et al. 1992). They show relatively uniform $\varepsilon Nd_{(0)}$ values (from − 17.1 to − 10.3; Table 4) and negative $\varepsilon Nd_{(530)}$ values, varying between − 11.3 and − 4.5 (Fig. 11). Nd TDM model ages were calculated according to DePaolo (1981), yielding Late Paleoproterozoic to Early Mesoproterozoic ages (1388–1897 Ma), with an average value at 1721 Ma, similar to those already published by López-Guijarro et al. (2008).

4 Discussion: type of basin model in which the Sierra Albarrana Group was deposited

The quite negative $\varepsilon Nd_{(530)}$ values (from − 11.3 to − 4.5; Table 4) calculated for the metasedimentary series of the Sierra Albarrana Group indicate a dominant input of terrigenous materials with an old continental crust affinity and limited contributions from juvenile sources. The geochemical compositions place the deposition in a continental active margin. Given the significant and increasing influence of the sedimentary processes and transport over the pelitic protoliths, and the recycled character of the terrigenous sediments, the conditions would have probably evolved to those of a passive margin. Both $\varepsilon Nd_{(530)}$ and $f^{Sm/Nd}$ values (from − 0.445 to − 0.346; Table 4) are compatible with those proposed by McLennan and Hemming (1992) for sedimentary rocks deposited in tectonic settings sharing continental active margin and passive margin/cratonic features. The geochemical composition of our samples (Figs. 9, 10) points to the same direction. The negative $\varepsilon Nd_{(530)}$ and geochemical features such as Th/U, Th/Sc, and Eu/Eu*, account for a significant sedimentary maturity and recycled

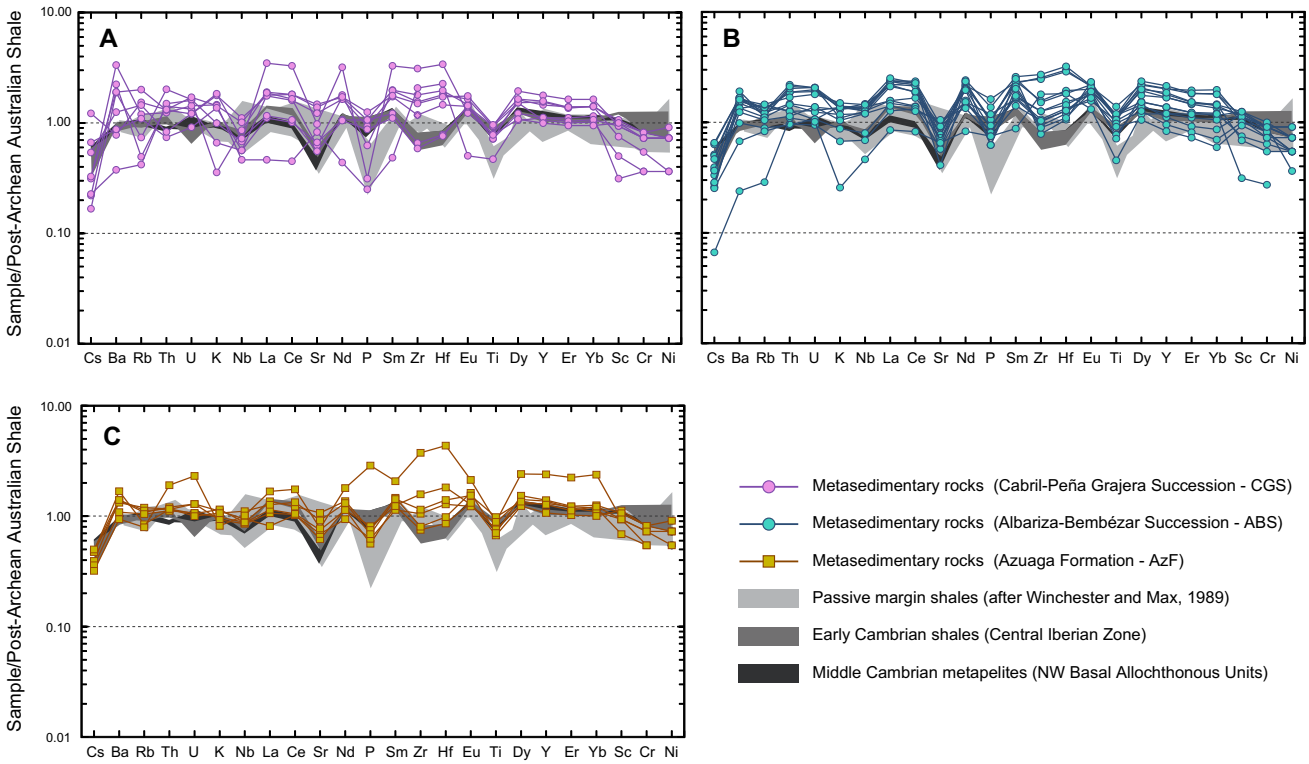

Fig. 9 PAAS-normalized trace elements multi-variation diagrams of the Early Cambrian metasedimentary series of the Sierra Albarrana Group (SW Iberian Autochthonous Domain). **a** Metasedimentary rocks from Cabril-Peña Grajera Succession (CGS); **b** Metasedimentary rocks from Albariza-Bembézar Succession (ABS); **c** Metasedimentary rocks from Azuaga Formation (AzF). PAAS after Taylor and McLennan (1985). Passive margin shales (after Winchester and Max 1989), Early Cambrian shales from Central Iberian Zone (Fuenlabrada et al. 2016), and Middle Cambrian metapelitic rocks from NW Basal Allochthonous Units (Fuenlabrada et al. 2012) fields have been included for comparison (see the text for a further explanation)

character (McLennan et al. 1993), favouring a provenance from old and reworked continental upper crust materials with an evident felsic contribution. The metasedimentary rocks from Sierra Albarrana Group display uniform Sm/Nd ratios, which suggests an intense recycling history and a limited contribution from differentiated sources. These samples show Nd-isotope features quite different from those found in typical arc-related rocks, with variable Sm/Nd ratios and positive εNd (e.g., metasedimentary series in the NW Upper Allochthonous Units; Fuenlabrada et al. 2010, 2020). As mentioned before, the rest of geochemical proxies indicate a reworking of detrital materials with a high influence of the sedimentary transport, and likely linked to a continental active margin or an incipient passive margin. This is also confirmed by the comparison with a wide range of geochemical indicators used by Bhatia and Crook (1986) to constrain the affinity with certain geodynamic scenarios. Considering Nd model ages in siliciclastic rocks as a weighted average of contributions with a different age and provenance, potentially derived from nearby surrounding source areas and/or, according to some authors areas located thousands of kilometres away (e.g., Avigad et al. 2003; Morag et al. 2011), the here presented very old Nd model ages (avg. 1721 Ma; Table 4; Fig. 11) account for a limited and variable mixing with juvenile detrital materials coming from the outermost part of the active margin and magmatic arc sources, and suggest a dominant input from older basement sections. The closeness of the paleobasins of the Ediacaran sedimentary sequences from the Serie Negra Group to the Cadomian magmatic arc define specific and identifiable geochemical features (Rojo-Pérez et al. 2019 and submitted), although their Nd model ages do not mirror significant juvenile contributions from the magmatic activity, with constant and old TDM ages with an old crustal affinity from a Cadomian basement provenance (Rojo-Pérez et al. submitted). The geochemical and isotope data here presented for the Sierra Albarrana Group suggest that their sedimentary protoliths were not laid down coevally with ongoing magmatism, at least not close to a magmatic axis, since there is no geochemical evidence for a significant influence of the arc-system over the geochemical features in the whole group of rocks from Sierra Albarrana. In this regard, the recycling of an old (Paleoproterozoic) basement into newly-formed igneous rocks that were eroded from the arc-system

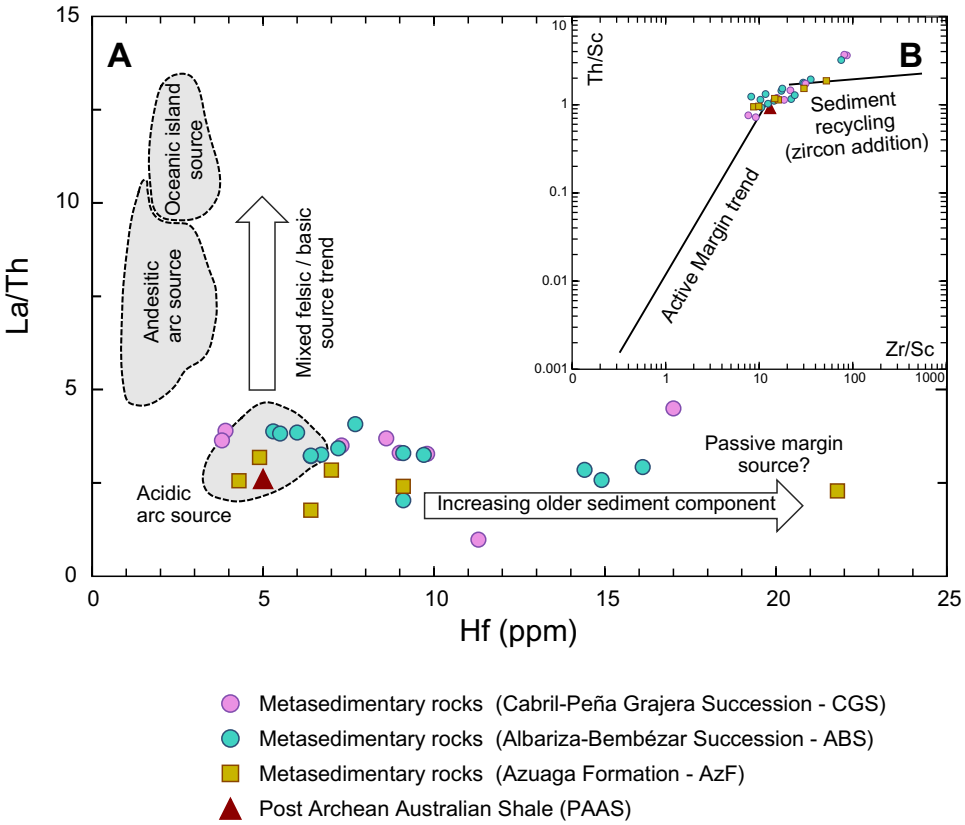

Fig. 10 **a** La/Th vs. Hf diagram for active/passive margin source discrimination of sandstones (fields from Floyd and Leveridge 1987; and references therein). **b** Th/Sc vs. Zr/Sc diagram (after McLennan et al. 1993). Samples plot away from igneous compositional variations, suggestive of an increase in sedimentary sorting and recycling

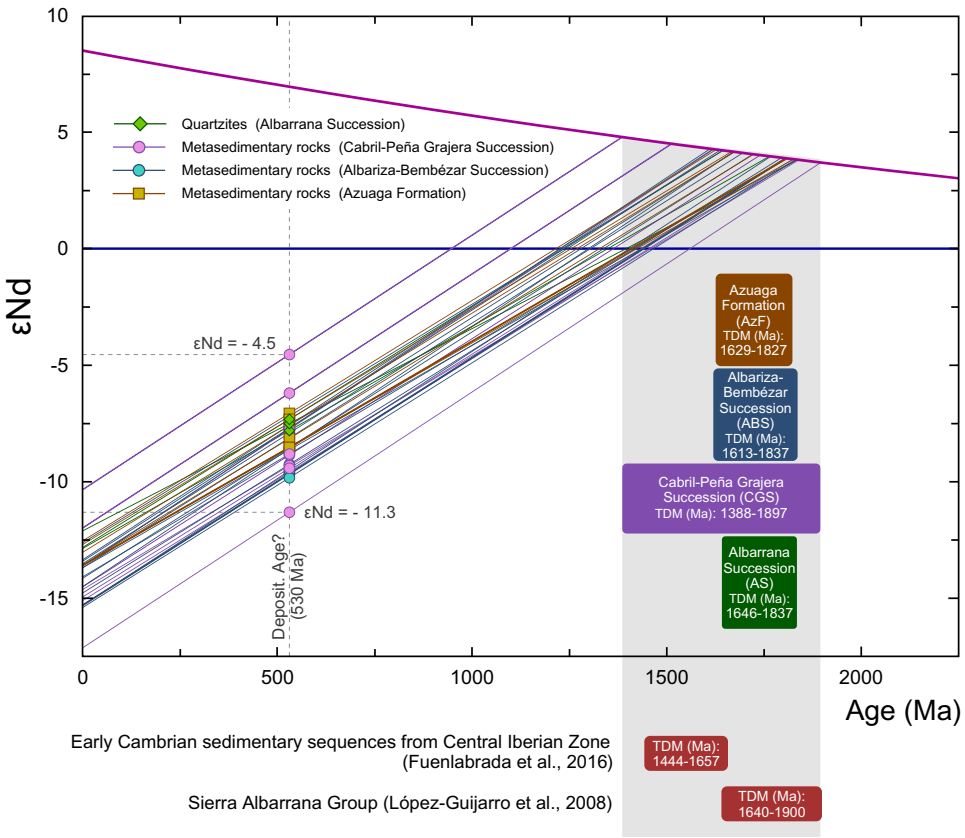

Fig. 11 TDM model ages (after DePaolo 1981) of the Early Cambrian metasedimentary series from the Sierra Albarrana Group (SW Iberian Autochthonous Domain). TDM model ages of Early Cambrian metasedimentary sequences from Central Iberian Zone (Fuenlabrada et al. 2016), and TDM model ages of Sierra Albarrana Group (López-Guijarro et al. 2008) have been included for comparison

should be considered a rather minor contributor, unlike what might have happened with the coeval Ediacaran–Cambrian Malcocinado volcanoclastic series, with Nd-isotope features more in line with a greater influence of the magmatic activity of the Cadomian arc (López-Guijarro et al. 2008). All these geochemical and isotopic characteristics match those found in the Early Cambrian sedimentary sequences of the autochthonous section of the Central Iberian Zone (Pusa shales Formation—Upper Unit), which show, in average values, slightly less negative $\varepsilon Nd_{(530)}$ (from − 5.2 to − 4.0) and younger TDM model ages (1444–1657 Ma; Fuenlabrada et al. 2016), although overlapping some individual values obtained in the autochthonous section of the Sierra Albarrana Group (Fig. 11). Homogeneous geochemical data of the Early Cambrian sedimentary sequences in Central Iberian Zone also support a high textural and mineralogical maturity compatible with old crustal materials, probably coming from a reworked continental source in an emerged Gondwanan hinterland location (Fuenlabrada et al. 2016). The Paleoproterozoic and Mesoproterozoic TDM model ages (Fig. 11) probably result from a mixing of limited Neoproterozoic and dominant Paleoproterozoic/Archean components, pointing to the denudation of an old continental crust (Paleoproterozoic basement), or a crust built at the expense of it, that was exposed during Early Cambrian times. This is compatible with an exposure of a Paleoproterozoic basement (e.g., in the Moroccan Meseta; Pereira et al. 2015) and/or erosion of old recycled continental crust. The increase in weathering indexes (CIA and PIA values; Table 2) in the metasedimentary rocks of the Albarrana Succession through to the Azuaga Formation is compatible with both possibilities.

Although our results are in agreement with those obtained by Lopez-Guijarro et al. (2008), who suggested common Archean/Paleoproterozoic old continental crust sources for the Serie Negra Group and the metasedimentary rocks of Sierra Albarrana during the latest Neoproterozoic, a Cambrian age for the sedimentary sequences of the Sierra Albarrana Group precludes a direct comparison with the Ediacaran Serie Negra Group. The most probable contributor for the detrital material was a Paleoproterozoic basement and/or an old recycled continental crust currently located in more eastern sections of the Gondwanan margin than those of the Serie Negra. The Tuareg Shield (Fig. 12b) shows abundant Paleoproterozoic and Archean source rocks with scarce Neoproterozoic and Mesoproterozoic ages (Brahimi et al. 2018), being probably the dominant contributor, through the Saharan platform, as previously suggested by Cambeses et al. (2017). These old recycled materials present Nd-isotope features comparable with those of the southern Central Iberian Zone (Fuenlabrada et al. 2016, 2020), what suggests easternmost locations for the Variscan autochthonous sections of the Iberian Massif (Bea et al. 2010; Talavera et al. 2013; Fernández-Suárez et al. 2014) (Fig. 12b).

Recent paleogeographic reconstructions of the peri-Gondwanan domain acknowledge that the autochthonous sections of the Variscan Orogen occupied inward positions across the margin of Gondwana relative to their respective allochthons (Díez Fernández et al. 2016). This reconstruction fits well with the orogen-scale distribution of paleogeographic domains of the Cadomian arc-system during the latest Ediacaran and Cambrian. The most external sections of the Cadomian arc-system, such as the fore-arc and arc, are preserved in the Variscan Upper Allochthon (Andonaegui et al. 2002; Díaz García et al. 2010; Fuenlabrada et al. 2010; Albert et al. 2015). The Variscan Ophiolitic and Basal allochthons include remnants of a Cadomian back-arc (Abati et al. 2010; Díez Fernández et al. 2010, 2016; Fuenlabrada et al. 2012; Andonaegui et al. 2017; Arenas et al. 2018, 2020; Sánchez Martínez et al. 2020), while in the autochthon were accumulated thick sedimentary series in the flank of that back-arc basin closer to the mainland in a differentiated lateral position (Rodríguez Alonso et al. 2004b, 2020; Pereira et al. 2012a; Fuenlabrada et al. 2016). Variscan subduction/accretion polarity for the peri-Gondwanan terranes of Iberia was directed toward Laurussia (i.e., to the W and SW in present-day coordinates; Díez Fernández et al. 2016). Therefore, the current juxtaposition of Variscan allochthons on top of autochthons could be roughly translated in paleogeographic terms into a more internal position across the margin as we move down through the Variscan tectonic pile, and also as we move E or NE through the same allochthonous or autochthonous terrane. Accordingly, the position of the Sierra Albarrana Group to the SW of the Variscan autochthon widely exposed in the Central Iberian Zone would imply a position closer to the mainland for the latter, in a more eastern lateral location along the Gondwanan margin, closer to the Sahara Metacraton (Fig. 12b) (Bea et al. 2010; Talavera et al. 2012; Kromer and Romer 2013; Fernández-Suárez et al. 2014; Albert et al. 2015; Stephan et al. 2019b; Fuenlabrada et al. 2020).

Given the widespread angular unconformity between Ediacaran and Early Cambrian rocks that can be recognized across the Iberian Massif, topographic uplift must have played a role in the onset of Early Cambrian basins across the margin. Ediacaran thrusting (obduction) directed toward mainland Gondwana was responsible for the emplacement of peripheral (fore-arc) sections of the arc-system onto inboard sections of the Gondwana margin (Díez Fernández et al. 2019), which came along with coeval inversion (inland-verging folds; Díaz García et al. 2010) and across-margin segmentation (Villaseca et al. 2014) of back-arc Cadomian basins. Inland-directed obduction of peripheral sections of an arc-system together with inland-verging folds in the back-arc are strongly compatible with the development of a retro-arc (retro-foreland) basin over the back of the arc-system (Fig. 12a). In a convergent scenario, the interaction between

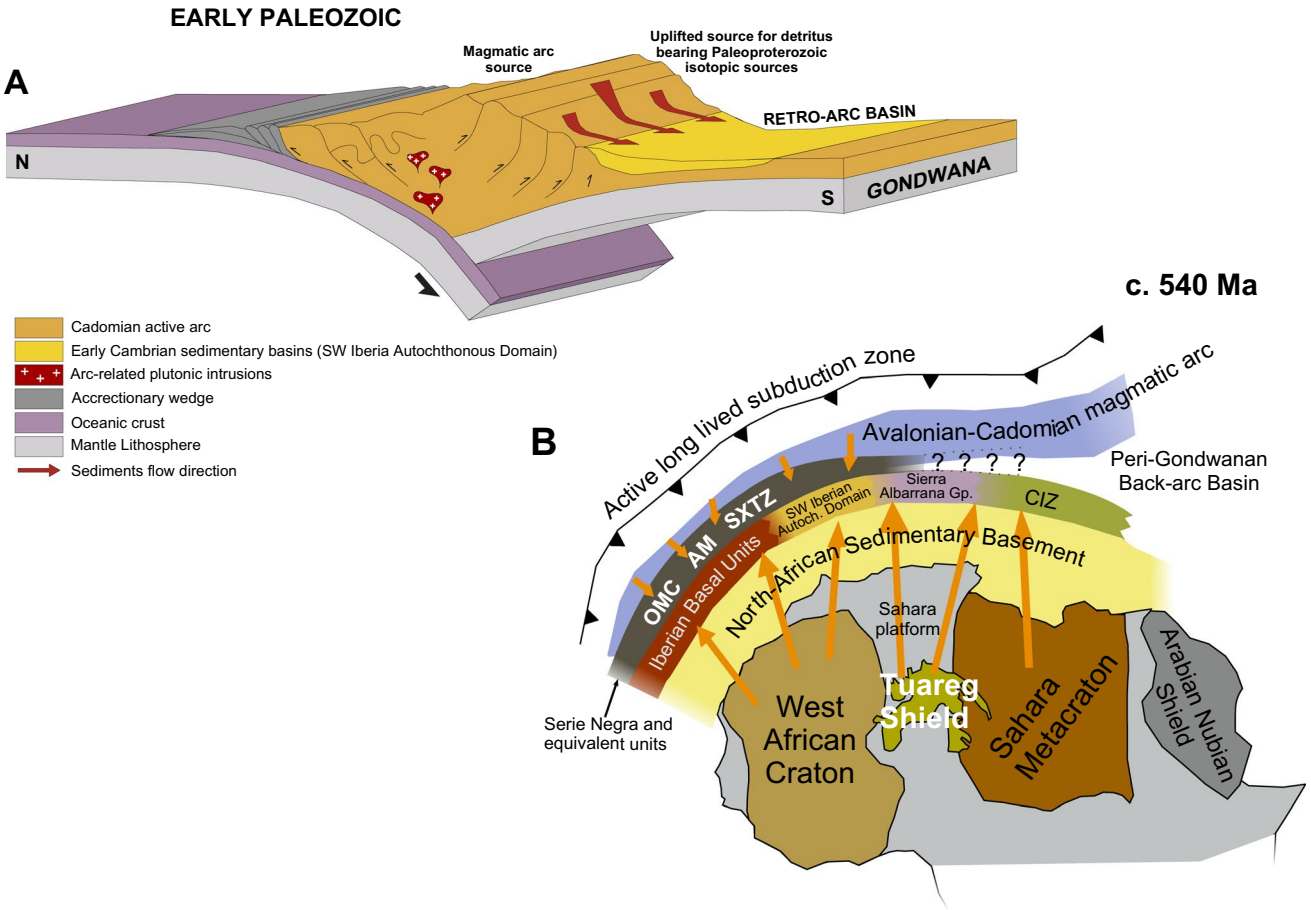

Fig. 12 **a** Simplified model (not to scale) of an Early Cambrian retro-arc basin for the SW Iberian Autochthonous Domain (Sierra Albarrana Group). **b** Schematic paleogeographic reconstruction model (not to scale) for the Gondwanan margin during the approximate Ediacaran–Cambrian transition (c. 540 Ma) (after Albert et al. 2015; Brahimi et al. 2018). Iberian sedimentary basins locations are shown in relation to the main North African cratonic masses. CIZ—Central Iberian Zone. OMC (Ossa-Morena Complex), AM (Armorican Massif), and SXTZ (Saxo-Thuringian Zone) locations according to Rojo-Pérez et al. submitted. Arrows show the probable provenance for the detrital materials (see text for further explanation)

the peri-Gondwanan trench and the external part of the continent during Neoproterozoic times resulted in widespread contraction (Díez Fernández et al. 2019), thus generating significant relief, either at the expense of the fore-arc, arc, or even the back-arc, which would have been the main detritus suppliers for a retro-arc basin. The more external Ediacaran–Cambrian paleoposition of the Variscan autochthonous section that is preserved in Sierra Albarrana relative to the rest of the Variscan autochthon that is preserved elsewhere to the N and NW, makes the Sierra Albarrana Group a good candidate to represent the infilling of a Cambrian retro-arc basin fed by detritus coming from tectonically uplifted sections of the arc and fore-arc, as this would be a domain of the Ediacaran back-arc of the autochthon rather close to the uplifted sections. All the geochemical features of those sequences presented in this work are fully compatible with this interpretation.

The distribution of siliciclastic materials within the Sierra Albarrana sedimentary basin follows predictable models for the evolution in foreland basins, where the sedimentary sequences record long-term climatic and tectonic changes (Armitage et al. 2011). The presence of *Skolithos*, *Monocraterion*, and *Arenicolites* in the Albarrana Succession indicates a shallow marine environment for the deposition of this series (Azor et al. 1991), possibly in a bulge section. In the Cabril-Peña Grajera and Albariza-Bembézar successions, the flysch-type deposits, with relatively immature sediments and turbiditic character, could be the result of deepening in the retro-arc basin, possibly related to tectonically-induced subsidence in a fore-deep section. The greater influence of the sedimentary transport, as suggested by the increase in the geochemical maturity and recycling character of the metasedimentary record in the Albariza-Bembézar Succession and Azuaga Formation could be related to a widening of the basin, what would have heralded the terminal stages

of contraction in the upper plate, where the continuous input of recycled sediments from old basement sources filled the basin in a more stable environment such as is the case of the intertidal zone deposits in a marine platform suggested for the Azuaga Formation (Insúa et al. 1990; González del Tánago 1995; and references therein).

5 Main conclusions

Nd-isotope data from metasedimentary series of the Sierra Albarrana Group (SW Iberian Autochthonous Domain) are compatible with old reworked materials with continental crust affinity and limited contributions from juvenile sources. This, together with a high recycling character of the terrigenous sediments place the basins within an active margin sharing geochemical features with the initial stages of a passive margin. The geochemical and isotopic features of the Sierra Albarrana Group are similar to those found in the sedimentary sequences of the autochthonous section of the Central Iberian Zone, which implies a comparable depositional setting during their sedimentation in Early Paleozoic times and a close paleolocation of their sedimentary basins, but in an easternmost location along the Gondwanan margin (Tuareg Shield—Sahara Metacraton). The progressive denudation of a Paleoproterozoic basement or a recycled continental crust was the dominant source for the recycled materials with old Nd model ages found in the metasedimentary sequences in Sierra Albarrana. The exposure of this old crustal section after topographic uplift was caused by an Ediacaran inland-directed thrusting, which emplaced fore-arc sections of the arc-system onto inboard sections of the Gondwanan margin. This contractive scenario during latest Neoproterozoic times caused that these uplifted arc and fore-arc sections were the dominant detrital contributors for the filling of a retro-arc basin, which is considered as the most probable setting for the deposit of the Sierra Albarrana sedimentary rocks in Early Cambrian times.

Acknowledgements This work is dedicated to the extensive career that Professor Carmen Galindo devoted to Geology, and more particularly to Isotope Geochemistry, carrying out for over 25 years an invaluable work as head of the Geochronology and Isotope Geochemistry Service (Universidad Complutense de Madrid). She was also an inspiration to Geology students who decided devote their scientific career to the fascinating field of Geochemistry. We would like to acknowledge the invaluable help of the editor Pilar Montero, as well as the insightful and constructive contributions made by Aitor Cambeses and another anonymous reviewer that has resulted in an improved version of the manuscript. Financial support has been provided by the Spanish project CGL2016-76438-P (Ministerio de Economía Industria y Competitividad). This work is a contribution to IGCP project 683 (Pre-Atlantic geological connections among northwest Africa, Iberia and eastern North America: Implications for continental configurations and economic resources).

References

Ábalos, B., Eguiluz, L., & Apalategui, O. (1990). Constitución tectonoestratigráfica del Corredor Blastomilonítico de Badajoz - Córdoba: nueva propuesta de subdivisión. *Geogaceta, 7,* 71–73.

Ábalos, B., Gil Ibarguchi, J. I., Sánchez-Lorda, M. E., & Paquette, J. L. (2012). African/Amazonian proterozoic correlations of Iberia: a detrital zircon U–Pb study of early Cambrian conglomerates from the Sierra de la Demanda (Northern Spain). *Tectonics, 31,* TC3003. https://doi.org/10.1029/2011TC003041.

Abati, J., Arenas, R., Díez Fernández, R., Albert, R., & Gerdes, A. (2018). Combined zircon U–Pb and Lu–Hf isotopes study of magmatism and high-P metamorphism of the basal allochthonous units in the SW Iberian Massif (Ossa-Morena complex). *Lithos, 322,* 20–37.

Abati, J., Gerdes, A., Fernández-Suárez, J., Arenas, R., Whitehouse, M. J., & Díez Fernández, R. (2010). Magmatism and early-Variscan continental subduction in the northern Gondwana margin recorded in zircons from the basal units of Galicia, NW Spain. *Geological Society of America Bulletin, 122,* 219–235. https://doi.org/10.1130/B26572.1.

Abbo, A., Avigad, D., Gerdes, A., & Güngör, T. (2015). Cadomian basement and Paleozoic to Triassic siliciclastics of the Taurides (Karacahisar dome, south-central Turkey): paleogeographic constraints from U–Pb–Hf in zircons. *Lithos, 227,* 122–139. https://doi.org/10.1016/j.lithos.2015.03.023.

Albert, R., Arenas, R., Gerdes, A., Sánchez Martínez, S., Fernández-Suárez, J., & Fuenlabrada, J. M. (2015). Provenance of the Variscan Upper Allochthon (Cabo Ortegal complex, NW Iberian Massif). *Gondwana Research., 28,* 1434–1448. https://doi.org/10.1016/j.gr.2014.10.016.

Alvarez Nava, H., García Casquero, J. L., Gil Toja, A., Hernández Urroz, J., Lorenzo Alvarez, S., López Díaz, F., et al. (1988). Unidades litoestratigráficas de los materiales Precámbrico-Cámbricos en la mitad suroriental de la Zona Centro-Ibérica. *II Congreso Geológico de España, SGE, Granada, 1,* 19–22.

Andonaegui, P., Abati, J., & Díez Fernández, R. (2017). Late Cambrian magmatic arc activity in peri-Gondwana: Geochemical evidence from metagranitoid rocks of the Basal Allochthonous Units of NW Iberia. *Geologica Acta, 15*(4), 305–321. https://doi.org/10.1344/GeologicaActa2017.15.4.4.

Andonaegui, P., Arenas, R., Albert, R., Sánchez Martínez, S., Díez Fernández, R., & Gerdes, A. (2016). The last stages of the Avalonian-Cadomian arc in NW Iberian Massif: Isotopic and igneous record for a long-lived peri-Gondwanan magmatic arc. *Tectonophysics, 681,* 6–14. https://doi.org/10.1016/j.tecto.2016.02.032.

Andonaegui, P., González del Tánago, J., Arenas, R., Abati, J., Martínez Catalán, J.R., Peinado, M. & Díaz García, F., (2002). Variscan-Appalachian Dynamics: The Building of the Late Paleozoic Basement. In J.R. Martínez Catalán, R.D. Hatcher, R. Arenas & F. Díaz García, (Eds.), *Tectonic setting of the Monte Castelo gabbro (Ordenes Complex, northwestern Iberian Massif): Evidence for an arc-related terrane in the hanging wall to the Variscan suture*. Geological Society of America (pp. 37–56), 364. https://doi.org/10.1130/0-8137-2364-7.37.

Apalategui, O., Borrero, J., & Higueras, P. (1985). División en grupos de rocas en Sierra Morena Oriental. *Colección Temas Geológico-Mineros, 2,* 73–80.

Arenas, R., Díez Fernández, R., Rubio Pascual, F. J., Sánchez Martínez, S., Martín Parra, L. M., Matas, J., et al. (2016b). The Galicia–Ossa-Morena zone: Proposal for a new zone of the Iberian Massif. Variscan implications. *Tectonophysics, 681*, 135–143. https://doi.org/10.1016/j.tecto.2016.02.030.

Arenas, R., Díez Fernández, R., Sánchez Martínez, S., Gerdes, A., Fernández-Suárez, J., & Albert, R. (2014). Two-stage collision:

exploring the birth of Pangea in the Variscan terranes. *Gondwana Research, 25,* 756–763. https://doi.org/10.1016/j.gr.2013.08.009.

Arenas, R., Fernández-Suárez, J., Montero, P., Díez Fernández, R., Andonaegui, P., Sánchez Martínez, S., et al. (2018). The Calzadilla Ophiolite (SW Iberia) and the Ediacaran fore-arc evolution of the African margin of Gondwana. *Gondwana Research, 58,* 71–86. https://doi.org/10.1016/j.gr.2018.01.015.

Arenas, R., Gil Ibarguchi, J. I., González Lodeiro, F., Klein, E., Martínez Catalán, J. R., Ortega Gironés, E., et al. (1986). Tectonostratigraphic units in the complexes with mafic and related rocks of the NW of the Iberian Massif. *Hercynica, 2,* 87–110.

Arenas, R., Sánchez Martínez, S., Albert, R., Haissen, F., Fernández-Suárez, J., Pujol-Solà, N., Andonaegui, P., Díez Fernández, R., Proenza, J.A., García-Casco, A. & Gerdes, A., (2020). 100 myr cycles of oceanic lithosphere generation in peri-Gondwana: Neoproterozoic–Devonian ophiolites from the NW African–Iberian margin of Gondwana and the Variscan Orogen. Geological Society, London, Special Publications (pp. 503) https://doi.org/10.1144/SP503-2020-3.

Arenas, R., Sánchez Martínez, S., Díez Fernández, R., Gerdes, A., Abati, J., Fernández-Suárez, J., et al. (2016a). Allochthonous terranes involved in the Variscan suture of NW Iberia: A review of their origin and tectonothermal evolution. *Earth-Science Reviews*, *161*, 140–178. https://doi.org/10.1016/j.earscirev.2016.08.010.

Armitage, J., Duller, R., Whittaker, A., & Allen, P. A. (2011). Transformation of tectonic and climatic signals from source to sedimentary archive. *Nature Geoscience, 4,* 231–235. https://doi.org/10.1038/ngeo1087.

Armstrong-Altrin, J. S., Lee, Y. I., Verma, S. P., & Ramasamy, S. (2004). Geochemistry of sandstones from the upper Miocene Kudankulam formation, southern India: Implications for provenance, weathering, and tectonic setting. *Journal of Sedimentary Research, 74,* 285–297. https://doi.org/10.1306/082803740285.

Avigad, D., Gerdes, A., Morag, N., & Bechstädt, T. (2012). Coupled U–Pb–Hf of detrital zircons of Cambrian sandstones from Morocco and Sardinia: Implications for provenance and Precambrian crustal evolution of North Africa. *Gondwana Research, 21,* 690–703. https://doi.org/10.1016/j.gr.2011.06.005.

Avigad, D., Kolodner, K., McWilliams, M., Persing, H., & Weissbrod, T. (2003). Origin of northern Gondwana Cambrian sandstone revealed by detrital zircon SHRIMP dating. *Geology, 31*(3), 227–230. https://doi.org/10.1130/0091-7613(2003)031%3c0227:OONGCS%3e2.0.CO;2.

Avigad, D., Rossi, Ph., Gerdes, A., & Abbo, A. (2018). Cadomian metasediments and Ordovician sandstone from Corsica: Detrital zircon U–Pb–Hf constrains on their provenance and paleogeography. *International Journal of Earth Sciences (Geol Rundsch), 107,* 2803–2818. https://doi.org/10.1007/s00531-018-1629-3.

Azor, A., (1994). Evolución tectonometamórfica del límite entre las zonas Centroibérica y de Ossa-Morena (Cordillera Varisca, SO de España) (PhD thesis) Universidad de Granada, Spain (pp. 295).

Azor, A., & Ballèvre, M. (1997). Low-pressure metamorphism in the Sierra Albarrana Area (Variscan Belt, Iberian Massif). *Journal of Petrology, 38*(1), 35–64. https://doi.org/10.1093/petroj/38.1.35.

Azor, A., Expósito, I., González Lodeiro, F., Simancas, J. F., & Martínez Poyatos, D. (2004). La Unidad de Sierra Albarrana. In J. A. Vera (Ed.), *Geología de España* (pp. 182–186). Madrid: SGE-IGME.

Azor, A., González Lodeiro, F., Marcos, A., & Simancas, J. F. (1991). Edad y estructura de las rocas de Sierra Albarrana (SW del Macizo Hespérico). Implicaciones regionales. *Geogaceta, 10,* 119–124.

Azor, A., Lodeiro, F. G., & Simancas, J. F. (1994). Tectonic evolution of the boundary between the central Iberian and the Ossa-Morena zones (Variscan belt, southwest Spain). *Tectonics, 13,* 45–61. https://doi.org/10.1029/93TC02724.

Azor, A., Simancas, J. F., Martínez Poyatos, D. J., Montero, P., González Lodeiro, F., & Gabites, J. (2012). Nuevos datos geocronológicos sobre la evolución tectonometamórfica de la Unidad de Sierra Albarrana (Zona de Ossa-Morena, SO de Iberia). *Geo-Temas, 13,* 341–344.

Azor, A., Simancas, J. F., Martínez Poyatos, D. J., Montero, P., González Lodeiro, F., & Pérez-Cáceres, I. (2016). U–Pb zircon age and tectonic meaning of the Cardenchosa pluton (Ossa-Morena Zone). *Geo-Temas, 2,* 23–26.

Ballèvre, M., Le Goff, E., & Hébert, R. (2001). The tectonothermal evolution of the Cadomian belt of northern Brittany, France: A Neoproterozoic volcanic arc. *Tectonophysics, 331*(1–2), 19–43. https://doi.org/10.1016/S0040-1951(00)00234-1.

Bandrés, A., (2001). Evolución geodinámica poliorogénica de los dominios septentrionales de la ZOM. Universidad del País Vasco, Tesis Doctoral (pp. 377).

Bea, F., Montero, P., Talavera, C., Abu Anbar, M., Scarrow, J., Molina, J. F., & Moreno, J. A. (2010). The palaeogeographic position of Central Iberia in Gondwana during the Ordovician: Evidence from zircon geochronology and Nd isotopes. *Terra Nova, 22,* 341–346. https://doi.org/10.1111/j.1365-3121.2010.00957.x.

Bhatia, M. R., & Crook, K. A. W. (1986). Trace element characteristics of graywackes and tectonic setting discrimination of sedimentary basins. *Contributions to Mineralogy and Petrology, 92,* 181–193. https://doi.org/10.1007/BF00375292.

Brahimi, S., Liégeois, J. P., Ghienne, J. F., Munschy, M., & Bourmatte, A. (2018). The Tuareg shield terranes revisited and extended towards the northern Gondwana margin: Magnetic and gravimetric constraints. *Earth-Science Reviews, 185,* 572–599. https://doi.org/10.1016/j.earscirev.2018.07.002.

Cambeses, A., Scarrow, J. H., Montero, P., Lázaro, C., & Bea, F. (2017). Palaeogeography and crustal evolution of the Ossa-Morena Zone, southwest Iberia, and the North Gondwana margin during the Cambro–Ordovician: A review of isotopic evidence. *International Geology Review, 59,* 94–130. https://doi.org/10.1080/00206814.2016.1219279.

Carvalhosa, A. (1965). Contribuição para o conhecimento geológico da região entre Portel e Ficalho (Alentejo). Memorias dos Serviços Geológicos de Portugal. *Nova Série, 11,* 1–32.

Chacón, J., Delgado Quesada, M., & Garrote, A. (1974). Sobre la existencia de dos diferentes dominios de metamorfismo regional en la banda Elvas-Badajoz-Córdoba. *Boletín Geológico y Minero, 85,* 713–717.

Collett, S., Schulmann, K., Štípská, P., & Míková, J. (2020). Chronological and geochemical constraints on the pre-variscan tectonic history of the Erzgebirge, Saxothuringian Zone. *Gondwana Research, 79,* 27–48. https://doi.org/10.1016/j.gr.2019.09.009.

Condie, K. C. (1993). Chemical composition and evolution of the upper continental crust: Contrasting results from surface samples and shales. *Chemical Geology, 104,* 1–37. https://doi.org/10.1016/0009-2541(93)90140-E.

Condie, K. C., Dengate, J., & Cullers, R. L. (1995). Behavior of rare earth elements in a paleoweathering profile on granodiorite in the Front Range, Colorado, USA. *Geochimica et Cosmochimica Acta, 59*(2), 279–294. https://doi.org/10.1016/0016-7037(94)00280-Y.

Cox, R., Lowe, D. R., & Cullers, R. L. (1995). The influence of sediment recycling and basement composition on evolution of mudrock chemistry in the southwestern United States. *Geochimica et Cosmochimica Acta, 59*(14), 2919–2940. https://doi.org/10.1016/0016-7037(95)00185-9.

Cullers, R. L. (1994). The controls on the major and trace element variation of shales, siltstones and sandstones of Pennsylvanian-Permian age from uplifted continental blocks in Colorado to

platform sediment in Kansas, USA. *Geochimica et Cosmochimica Acta, 58,* 4955–4972. https://doi.org/10.1016/0016-7037(94)90224-0.

Cullers, R. L. (2002). Implications of elemental concentrations for provenance, redox conditions, and metamorphic studies of shales and limestones near Pueblo, CO, USA. *Chemical Geology, 191,* 305–327. https://doi.org/10.1016/S0009-2541(02)00133-X.

Dallmeyer, R. D., Martínez Catalán, J. R., Arenas, R., Gil Ibarguchi, J. I., Gutiérrez Alonso, G., Farias, P., et al. (1997). Diachronous Variscan tectonothermal activity in the NW Iberian Massif: Evidence from $^{40}Ar/^{39}Ar$ dating of regional fabrics. *Tectonophysics, 277,* 307–337. https://doi.org/10.1016/S0040-1951(97)00035-8.

Dallmeyer, R. D., & Quesada, C. (1992). Cadomian vs. Variscan evolution of the Ossa-Morena zone (SW Iberia): Field and $^{40}Ar/^{39}Ar$ mineral age constrains. *Tectonophysics, 216,* 339–364. https://doi.org/10.1016/0040-1951(92)90405-U.

Delgado Quesada, M. (1971). Esquema geológico de la Hoja núm. 878 de Azuaga, Badajoz. *Boletín Geológico y Minero, 82,* 277–286.

Delgado Quesada, M., Liñán, E, Pascual, E, & Pérez-Lorente, F. (1977). Criterios para la diferenciación de Dominios en Sierra Morena Central. *Studia Geologica Salmanticensia, 12,* 75–90.

DePaolo, D. J. (1981). Neodymium isotopes in the Colorado front range and crustal–mantle evolution in the Proterozoic. *Nature, 291,* 193–196. https://doi.org/10.1038/291193a0.

DePaolo, D. J. (1983). The mean life of continents: Estimates of continent recycling rates from Nd and Hf isotopic data and implications for mantle structure. *Geophysical Research Letters, 10,* 705–708. https://doi.org/10.1029/GL010i008p00705.

Díaz García, F., Sánchez Martínez, S., Castiñeiras, P., Fuenlabrada, J. M., & Arenas, R. (2010). A peri-Gondwanan arc in NW Iberia. II: Assessment of the intra-arc tectonothermal evolution through U–Pb SHRIMP dating of mafic dykes. *Gondwana Research, 17,* 352–362. https://doi.org/10.1016/j.gr.2009.09.010.

Díez Fernández, R., & Arenas, R. (2015). The Late Devonian Variscan suture of the Iberian Massif: A correlation of high-pressure belts in NW and SW Iberia. *Tectonophysics, 654,* 96–100. https://doi.org/10.1016/j.tecto.2015.05.001.

Díez Fernández, R., Arenas, R., Francisco Pereira, M., Sánchez Martínez, S., Albert Roper, R., Martín Parra, L. M., et al. (2016). Tectonic evolution of Variscan Iberia: Gondwana–Laurussia collision revisited. *Earth-Science Reviews, 162,* 269–292. https://doi.org/10.1016/j.earscirev.2016.08.002.

Díez Fernández, R., Fuenlabrada, J. M., Chichorro, M., Pereira, M. F., Sánchez Martínez, S., Silva, J. B., & Arenas, R. (2017). Geochemistry and tectonostratigraphy of the basal allochthonous units of SW Iberia (Évora Massif, Portugal): Keys to the reconstruction of pre-Pangean paleogeography in southern Europe. *Lithos, 268–271,* 285–301. https://doi.org/10.1016/j.lithos.2016.10.031.

Díez Fernández, R., Jiménez-Díaz, A., Arenas, R., Pereira, M. F., & Fernández-Suárez, J. (2019). Ediacaran obduction of a fore-arc ophiolite in SW Iberia: A turning point in the evolving geodynamic setting of peri-Gondwana. *Tectonics, 38,* 95–119. https://doi.org/10.1029/2018TC005224.

Díez Fernández, R., Martínez Catalán, J. R., Gerdes, A., Abati, J., Arenas, R., & Fernández- Suárez, J. (2010). U–Pb ages of detrital zircons from the Basal allochthonous units of NW Iberia: Provenance and paleoposition on the northern margin of Gondwana during the Neoproterozoic and Paleozoic. *Gondwana Research, 18,* 385–399. https://doi.org/10.1016/j.gr.2009.12.006.

Drost, K., Gerdes, A., Jeffries, T., Linnemann, U., & Storey, C. (2011). Provenance of Neoproterozoic and early Paleozoic siliciclastic rocks of the Teplá-Barrandian unit (Bohemian Massif): Evidence from U–Pb detrital zircon ages. *Gondwana Research, 19,* 213–231. https://doi.org/10.1016/j.gr.2010.05.003.

Eguíluz, L., (1987). Petrogénesis de rocas ígneas y metamórficas en el Antiforme Burguillos-Monesterio, Macizo Ibérico Meridional, (PhD thesis) (pp. 694). Universidad del País Vasco.

Eguíluz, L., Gil Ibarguchi, J. I., Abalos, B., & Apraiz, A. (2000). Superposed Hercynian and Cadomian orogenic cycles in the Ossa-Morena zone and related areas of the Iberian Massif. *Geological Society of America Bulletin, 112*(9), 1398–1413. https://doi.org/10.1130/0016-7606(2000)112%3c1398:SHACOC%3e2.0.CO;2.

Farias, P., Gallastegui, G., González-Lodeiro, F., Marquínez, J., Martín Parra, L.M., Martínez Catalán, J.R., Pablo Maciá, J.G. de & Rodríguez Fernández, L.R., (1987). Aportaciones al conocimiento de la litoestratigrafía y estructura de Galicia central 1. Memórias da Faculdade de Ciências, Universidade do Porto (pp. 411–431).

Fedo, C. M., Nesbitt, H. W., & Young, G. M. (1995). Unravelling the effects of potassium metasomatism in sedimentary rocks and paleosols, with implications for paleoweathering conditions and provenance. *Geology, 23,* 921–924. https://doi.org/10.1130/0091-7613(1995)023%3c0921:UTEOPM%3e2.3.CO;2.

Fernández-Suárez, J., Corfu, F., Arenas, R., Marcos, A., Martínez Catalán, J. R., Díaz García, F., et al. (2002a). U–Pb evidence for a polyorogenic evolution of the HP-HT units of the NW Iberian Massif. *Contributions to Mineralogy and Petrology, 143,* 236–253. https://doi.org/10.1007/s00410-001-0337-2.

Fernández-Suárez, J., Díaz García, F., Jeffries, T. E., Arenas, R., & Abati, J. (2003). Constraints on the provenance of the uppermost allochthonous terrane of the NW Iberian Massif: Inferences from detrital zircon U–Pb ages. *Terra Nova, 15,* 138–144. https://doi.org/10.1046/j.1365-3121.2003.00479.x.

Fernández-Suárez, J., Gutiérrez-Alonso, G., & Jeffries, T. E. (2002b). The importance of along-margin terrane transport in northern Gondwana: Insights from detrital zircon parentage in Neoproterozoic rocks from Iberia and Brittany. *Earth and Planetary Science Letters, 204*(1–2), 75–88. https://doi.org/10.1016/S0012-821X(02)00963-9.

Fernández-Suárez, J., Gutiérrez-Alonso, G., Jenner, G. A., & Tubrett, M. N. (2000). New ideas on the Proterozoic-Early Paleozoic evolution of NW Iberia: Insights from U–Pb detrital zircon ages. *Precambrian Research, 102,* 185–206. https://doi.org/10.1016/S0301-9268(00)00065-6.

Fernández-Suárez, J., Gutiérrez-Alonso, G., Pastor-Galán, D., Hofmann, M., Murphy, J. B., & Linnemanm, U. (2014). The Ediacaran-Early Cambrian detrital zircon record of NW Iberia: Possible sources and paleogeographic constraints. *International Journal of Earth Sciences, 103*(5), 1335–1357. https://doi.org/10.1007/s00531-013-0923-3.

Floyd, P. A., & Leveridge, B. E. (1987). Tectonic environment of the Devonian Gramscatho Basin, South Cornwall: Framework mode and geochemical evidence from turbiditic sandstones. *Journal of the Geological Society, 144*(4), 531–542. https://doi.org/10.1144/gsjgs.144.4.0531.

Fralick, P. W., & Kronberg, B. I. (1997). Geochemical discrimination of clastic sedimentary rock sources. *Sedimentary Geology, 113*(1–2), 111–124. https://doi.org/10.1016/S0037-0738(97)00049-3.

Franke, W., (1989). Tectonostratigraphic units in the Variscan belt of central Europe. In R.D Dallmeyer (Ed.), *Terranes in the Circum-Atlantic Paleozoic Orogens* (pp. 67–90) Geological Society of America Special Paper. https://doi.org/10.1130/SPE230-p67.

Fricke, W., (1941). Die Geologie des Grenxebietes zwischen nordöstlicher Sierra Morena und Extremadura. Phd Thesis. University of Berlin (pp. 91) Berlin: Germany.

Fuenlabrada, J. M., Arenas, R., Díez Fernández, R., Sánchez Martínez, S., Abati, J., & López Carmona, A. (2012). Sm–Nd isotope geochemistry and tectonic setting of the metasedimentary rocks from the basal allochthonous units of NW Iberia (Variscan suture,

Galicia). *Lithos, 148,* 196–208. https://doi.org/10.1016/j.lithos.2012.06.002.

Fuenlabrada, J. M., Arenas, R., Sánchez Martínez, S., Díaz García, F., & Castiñeiras, P. (2010). A peri-Gondwanan arc in NW Iberia I: Isotopic and geochemical constraints on the origin of the arc—a sedimentary approach. *Gondwana Research., 17,* 338–351. https://doi.org/10.1016/j.gr.2009.09.007.

Fuenlabrada, J. M., Arenas, R., Sánchez Martínez, S., Díez Fernández, R., Pieren, A. P., Pereira, M. F., et al. (2020). Geochemical and isotopic (Sm–Nd) provenance of Ediacaran–Cambrian metasedimentary series from the Iberian Massif. Paleoreconstruction of the North Gondwana margin. *Earth-Science Reviews, 201,* 103079.

Fuenlabrada, J. M., Pieren, A. P., Díez Fernández, R., Sánchez Martínez, S., & Arenas, R. (2016). Geochemistry of the Ediacaran-Early Cambrian transition in Central Iberia: Tectonic setting and isotopic sources. *Tectonophysics, 681,* 15–30. https://doi.org/10.1016/j.tecto.2015.11.013.

Garcia, D., Coelho, J., & Perrin, M. (1991). Fractionation between TiO_2 and Zr as a measure of sorting within shale and sandstone series (Northern Portugal). *European Journal of Mineralogy, 3*(2), 401–414. https://doi.org/10.1127/ejm/3/2/0401.

Garrote, A. (1976). Asociaciones minerales del núcleo metamórfico de Sierra Albarrana (prov. de Córdoba). Sierra Morena Central. *Memorias e Noticias, publ Mus. Lab. Mineral. Geol. Univ. Coímbra, 82,* 17–39.

Garrote, A., Ortega Huertas, M. & Romero, J., (1980). Los yacimientos de pegmatitas de Sierra Albarrana (Provincia de Córdoba, Sierra Morena). 1ª Reunión sobre la geología de Ossa-Morena. Temas Geológicos Mineros (pp. 145–168) Madrid: IGME.

González del Tánago, J., (1995). El núcleo metamórfico de sierra albarrana y su campo de pegmatitas graníticas asociado, macizo Ibérico, Córdoba, España. Ediciós do Castro, Sada, serie Nova Terra 12 (pp. 511).

González del Tánago, J., & Arenas, R. (1991). Anfibolitas granatíferas de Sierra Albarrana (Córdoba). Termobarometría e implicaciones para el desarrollo del metamorfismo regional. *Revista de la Sociedad Geológica de España, 4,* 251–269.

González del Tánago, J., & Peinado, M. (1990). Contribución al estudio del metamorfismo de Sierra Albarrana (Z.O.M., Córdoba, España). *Boletín Geológico y Minero, 101,* 18–40.

Gutiérrez-Marco, J. C., San José, M. A. & Pieren, A. P. (1990) Central-Iberian Zone, Autochthonous sequences: Post-Cambrian Palaeozoic Stratigraphy. In R.D. Dallmeyer & E. Martínez García (Eds.), *Pre-Mesozoic Geology of Iberia* (pp. 160–171) Berlin: Springer. https://doi.org/10.1007/978-3-642-83980-1_14.

Henderson, B. J., Collins, W. J., Murphy, J. B., Gutierrez-Alonso, G., & Hand, M. (2016). Gondwanan basement terranes of the Variscan-Appalachian orogen: Baltican, Saharan and West African hafnium isotopic fingerprints in Avalonia, Iberia and the Armorican Terranes. *Tectonophysics, 681,* 278–304. https://doi.org/10.1016/j.tecto.2015.11.020.

Herron, M. M. (1988). Geochemical classification of terrigenous sands and shales from core or log data. *Journal of Sedimentary Research, 58,* 820–829. https://doi.org/10.1306/212F8E77-2B24-11D7-8648000102C1865D.

Hiscott, R. N. (1984). Ophiolitic source rocks for Taconic-age flysch: Trace-element evidence. *Geological Society of America Bulletin, 95,* 1261–1267. https://doi.org/10.1130/0016-7606(1984)95%3c1261:OSRFTF%3e2.0.CO;2.

Insúa, M., Carvajal, A., Huerta, J. & Matas, J., (1990). Memoria de la Hoja no 900 (La Cardenchosa). Mapa Geológico de España E. 1:50.000 (MAGNA), Segunda Serie, Primera edición. IGME (pp. 80). Depósito legal: M-22390-2007. ISBN: 978-84-7840-685-2

Jacobsen, S. B., & Wasserburg, G. J. (1980). Sm–Nd isotopic evolution of chondrites. *Earth and Planetary Science Letters, 50,* 139–155. https://doi.org/10.1016/0012-821X(80)90125-9.

Jensen, S., Palacios, T., & Eguíluz, L. (2004). Cambrian ichnofabrics from the Ossa Morena and Central Iberian zones: Preliminary results. *Geo-temas, 6*(2), 291–293.

Julivert, M., Fontboté, J.M., Ribeiro, A. & Conde, L., (1972). Mapa Tectónico de la Península Ibérica y Baleares E. 1:1.000.000. Instituto Geológico y Minero de España, Madrid. Depósito Legal: M-21994-1972.

Kroner, U., & Romer, R. L. (2013). Two plates—many subduction zones: The Variscan orogeny reconsidered. *Gondwana Research, 24,* 298–329. https://doi.org/10.1016/j.gr.2013.03.001.

Liñán, E., (1978). Bioestratigrafía de la Sierra de Córdoba [PhD]: Universidad de Granada (pp. 212).

Liñán, E. (1984). Los icnofósiles de la Formación Torreárboles (¿Precámbrico?-Cámbrico Inferior) en los alrededores de Fuente de Cantos, Badajoz. *Cuadernos do Laboratorio Xeoloxico de Laxe, 8,* 47–74.

Liñán, E., & Palacios, T. (1983). Aportaciones micropaleontológicas para el conocimiento del límite Precámbrico-Cámbrico en la Sierra de. Córdoba, España. *Comunicações dos Serviços Geológicos de Portugal, 69,* 227–234.

Liñán, E., Palacios, T., & Perejón, A. (1984). Precambrian–Cambrian boundary and correlation from southwestern and central part of Spain. *Geological Magazine, 121*(03), 221–228. https://doi.org/10.1017/S0016756800028284.

Liñán, E., & Quesada, C. (1990). Ossa-Morena Zone: 2. Stratigraphy. Rift phase. In R. D. Dallmeyer & E. Martínez García (Eds.), *Pre-mesozoic geology of Iberia* (pp. 259–266). Berlin: Springer.

Linnemann, U., Gerdes, A., Drost, K. & Buschmann, B., (2007). The continuum between Cadomian orogenesis and opening of the Rheic Ocean: Constraints from LA-ICP–MS U–Pb zircon dating and analysis of plate-tectonic setting (Saxo-Thuringian zone, northeastern Bohemian Massif, Germany). In U. Linnemann, R.D. Nance, P. Kraft & G. Zulauf (Eds.), *The evolution of the Rheic Ocean: From Avalonian–Cadomian Active Margin to Alleghenian–Variscan Collision*. 423. (pp. 61–96) Geological Society of America Special Paper. Boulder Colorado. https://doi.org/10.1130/2007.2423(03).

Linnemann, U., Gerdes, A., Hofmann, M., & Marko, L. (2014). The Cadomian Orogen: Neoproterozoic to Early Cambrian crustal growth and orogenic zoning along the periphery of the West African Craton—Constraints from U–Pb zircon ages and Hf isotopes (Schwarzburg Antiform, Germany). *Precambrian Research, 244,* 236–278. https://doi.org/10.1016/j.precamres.2013.08.007.

Linnemann, U., Pereira, F., Jeffries, T. E., Drost, K., & Gerdes, A. (2008). The Cadomian Orogeny and the opening of the Rheic Ocean: The diacrony of the geotectonic processes constrained by LA-ICP–MS U–Pb zircon dating (Ossa-Morena and Saxo-Thuringian zones, Iberian and Bohemian massifs). *Tectonophysics, 461*(1–4), 21–43. https://doi.org/10.1016/j.tecto.2008.05.002.

Linnemann, U., & Romer, R. L. (2002). The Cadomian Orogeny in Saxo-Thuringia, Germany: Geochemical and Nd–Sr–Pb isotopic characterization of marginal basins with constraints to geotectonic setting and provenance. *Tectonophysics, 352,* 33–64. https://doi.org/10.1016/S0040-1951(02)00188-9.

López Guijarro, R., (2006). Ambiente geodinámico y procedencia de las rocas sedimentarias precámbricas de las zonas de Ossa Morena y Centroibérica a través del análisis geoquímico. Boletín Geológico y Minero, 117 (Núm. Monográfico Especial): 499–505. ISSN: 0366-0176.

López Guijarro, R., Armendariz, M., Quesada, C., Fernández-Suárez, J., Murphy, J. B., Pin, C., & Bellido, F. (2008). Ediacaran-Palaeozoic tectonic evolution of the Ossa Morena and Central Iberian zones (SW Iberia) as revealed by Sm–Nd isotope systematics.

Tectonophysics, 461(1–4), 202–214. https://doi.org/10.1016/j.tecto.2008.06.006.

Lotze, F. (1945). Zur gliederung der varisziden der iberischen meseta. *Geotekt Forsch, 6,* 78–92.

Lugmair, G. W., & Marti, K. (1978). Lunar initial $^{143}Nd/^{144}Nd$ differential evolution of the lunar crust and mantle. *Earth and Planetary Science Letters, 39,* 349–357. https://doi.org/10.1016/0012-821X(78)90021-3.

IGME, (2015). Mapa geológico de España y Portugal E: 1.1000.000. Instituto Geológico y Minero de España, Madrid. Depósito Legal: M-35958-2014

Marcos, A., Azor, A., González Lodeiro, F., & Simancas, F. (1991). Early Phanerozoic trace fossils from the Sierra Albarrana Quartzites (Ossa-Morena Zone, Southwest Spain). *Scripta Geologica, 97,* 47–53.

Martín Parra, L. M., González Lodeiro, F., Martínez Poyatos, D., & Matas, J. (2006). The Puente Génave-Castelo de Vide Shear Zone (southern Central Iberian Zone, Iberian Massif): geometry, kinematics and regional implications. *Bulletin de la Société Géologique de France, 177,* 191–202. https://doi.org/10.2113/gssgfbull.177.4.191.

Martínez Catalán, J. R., Arenas, R., Abati, J., Sánchez Martínez, S., Díaz García, F., Fernández-Suárez, J., et al. (2009). A rootless suture and the loss of the roots of a mountain chain: The Variscan belt of NW Iberia. *Comptes Rendus Geoscience, 341*(2–3), 114–126. https://doi.org/10.1016/j.crte.2008.11.004.

Martínez Catalán, J. R., Arenas, R., Díaz García, F., & Abati, J. (1997). Variscan accretionary complex of northwest Iberia: Terrane correlation and succession of tectonothermal events. *Geology, 25,* 1103–1106. https://doi.org/10.1130/0091-7613(1997)025%3c1103:VACONI%3e2.3.CO;2.

Martínez Catalán, J.R., Arenas, R., Díaz García, F., Gómez Barreiro, J., González Cuadra, P., Abati, J., Castiñeiras, P., Fernández-Suárez, J., Sánchez Martínez, S., Andonaegui, P., González Clavijo, E., Díez Montes, A., Rubio Pascual, F.J. & Valle Aguado, B., (2007). Space and time in the tectonic evolution of the northwestern Iberian Massif. Implications for the Variscan belt. In R.D. Hatcher, M.P. Carlson, J.H. Mcbride & J.R. Martínez Catalán (Eds.), *4-D Framework of Continental Crust*. (pp. 403–423) Geological Society of America Memoir, Boulder, Colorado. https://doi.org/10.1130/2007.1200(21).

Martínez Catalán, J. R., Collett, S., Schulmann, K., Aleksandrowski, P., & Mazur, S. (2020). Correlation of allochthonous terranes and major tectonostratigraphic domains between NW Iberia and the Bohemian Massif, European Variscan belt. *International Journal of Earth Sciences (Geol Rundsch), 109,* 1105–1131. https://doi.org/10.1007/s00531-019-01800-z.

Martínez Poyatos, D., (1997). Estructura del Borde Meridional de la Zona Centroibérica y su Relación con el Contacto entre las Zonas Centroibérica y de Ossa-Morena. Tesis Doct., Univ. Granada (pp. 222).

Matte, P. (1991). Accretionary history and crustal evolution of the Variscan belt in Western Europe. *Tectonophysics, 196,* 309–337. https://doi.org/10.1016/0040-1951(91)90328-P.

McLennan, S. M. (1989). Rare earth elements in sedimentary rocks: Influence of provenance and sedimentary processes. *Mineralogical Society of America, Review in Mineralogy, 21,* 169–200.

McLennan, S. M., & Hemming, S. (1992). Samarium/neodymium elemental and isotopic systematics in sedimentary rocks. *Geochimica et Cosmochimica Acta, 56*(3), 887–898. https://doi.org/10.1016/0016-7037(92)90034-G.

McLennan, S.M., Hemming, S.R., McDaniel, D.K. & Hanson, G.N., (1993). Geochemical approaches to sedimentation, provenance and tectonics. In M.J. Johnssons & A. Basu (Eds.), *Processes controlling the composition of clastic sediments*. Geological Society of America Spec. Pap. 284, (pp. 21–40). https://doi.org/10.1130/SPE284-p21.

McLennan, S. M., & Taylor, S. R. (1991). Sedimentary rocks and crustal evolution: tectonic settings and secular trends. *Journal of Geology, 99,* 1–21.

McLennan, S. M., Taylor, S. R., & Hemming, S. R. (2006). Composition, differentiation, and evolution of continental crust: constrains from sedimentary rocks and heat flow. In M. Brown & T. Rushmer (Eds.), *Evolution and differentiation of the continental crust* (pp. 92–134). Cambridge: Cambridge University Press.

Mielke, J.E., (1979). Composition of the Earth's crust and distribution of the elements. In: F. R. Siegel (Ed.), *Review of research on modern problems in geochemistry*. International Association for Geochemistry and Cosmochemistry. Earth Science Series No. 16. UNESCO Report SC/GEO/544/3, Paris, (pp. 13–37).

Moita, P., Munhá, J., Fonseca, P.E., Pedro, J., Tassinari, C.C.G., Araújo, A. & Palacios, T., (2005). Phase equilibria and geochronology of Ossa-Morena eclogites, XIV Semana de Geoquímica, VIII Congresso de Geoquímica dos Países de Língua Portuguesa, pp. 463-466.

Morag, N., Avigad, D., Gerdes, A., Belousova, E., & Harlavan, Y. (2011). Detrital zircon Hf isotopic composition indicates long-distance transport of North Gondwana Cambrian–Ordovician sandstones. *Geology, 39,* 955–958. https://doi.org/10.1130/G32184.1.

Murphy, J. B., & Nance, R. D. (1989). Model for the evolution of the Avalonian-Cadomian belt. *Geology, 17*(8), 735–738. https://doi.org/10.1130/0091-7613(1989)017%3c0735:MFTEOT%3e2.3.CO;2.

Nägler, T. F., Schiller, H. J., & Gebauer, D. (1995). Evolution of the Western European continental crust: implications from Nd and Pb isotopes in Iberian sediments. *Chemical Geology, 121,* 345–357. https://doi.org/10.1016/0009-2541(94)00129-V.

Nakamura, N. (1974). Determination of REE, Ba, Fe, Mg, Na and K in carbonaceous and ordinary chondrites. *Geochimica et Cosmochimica Acta, 38,* 757–775. https://doi.org/10.1016/0016-7037(74)90149-5.

Nance, R. D., Gutiérrez-Alonso, G., Keppi, J. D., Linnemann, U., Murphy, J. B., Quesada, C., et al. (2010). Evolution of the Rheic Ocean. *Gondwana Research, 17*(2–3), 194–222. https://doi.org/10.1016/j.gr.2009.08.001.

Nesbitt, H. W., & Young, G. M. (1982). Early Proterozoic climates and plate motions inferred from major element chemistry of lutites. *Nature, 299,* 715–717. https://doi.org/10.1038/299715a0.

O'Nions, R. K., Carter, S. R., Evensen, N. M., & Hamilton, P. J. (1979). Geochemical and cosmochemical applications of Nd isotope analysis. *Annual Review of Earth and Planetary Sciences, 7,* 11–38.

Ordoñez Casado, B., Gebauer, D., & Eguíluz, L. (2009). Zircon ion-probe dating the maximum age of deposition of the Montemolín succession (Lower Serie Negra) in the Ossa Morena Zone, Spain. *Macla, 11,* 137–138.

Ordóñez-Casado, B., Gebauer, D., & Eguiluz, L. (1998). SHRIMP age-constraints for the calc-alkaline volcanism in the Olivenza-Monesterio Antiform (Ossa-Morena, SW Spain). *Mineralogical Magazine, 62A*(2), 1112–1113. https://doi.org/10.1180/minmag.1998.62A.2.248.

Orejana, D., Merino Martínez, E., Villaseca, C., & Andersen, T. (2015). Ediacaran–Cambrian paleogeography and geodynamic setting of the Central Iberian Zone: Constraints from coupled U–Pb–Hf isotopes of detrital zircons. *Precambrian Research, 261,* 234–251. https://doi.org/10.1016/j.precamres.2015.02.009.

Pastor-Galán, D., Gutiérrez-Alonso, G., Fernández-Suárez, J., Murphy, J. B., & Nieto, F. (2013). Tectonic evolution of NW Iberia during the Paleozoic inferred from the geochemical record of detrital

rocks in the Cantabrian Zone. *Lithos, 182–183,* 211–228. https://doi.org/10.1016/j.lithos.2013.09.007.

Pereira, M. F. (2015). Potential sources of Ediacaran strata of Iberia: A review. *Geodinamica Acta, 27*(1), 1–14. https://doi.org/10.1080/09853111.2014.957505.

Pereira, M. F., Chichorro, M., Linnemann, U., Eguiluz, L., & Silva, J. B. (2006). Inherited arc signature in Ediacaran and Early Cambrian basins of the Ossa-Morena Zone (Iberian Massif, Portugal): Paleogeographic link with European and North African Cadomian correlatives. *Precambrian Research, 144*(3–4), 297–315. https://doi.org/10.1016/j.precamres.2005.11.011.

Pereira, M.F., Chichorro, M., Williams, I.S. & Silva, J.B., (2008). Zircon U–Pb geochronology of paragneisses and biotite granites from the SW Iberian Massif (Portugal): Evidence for a paleogeographic link between the Ossa-Morena Ediacaran basins and the West African craton. In: J.P. Liégeois & E. Nasser (Eds.), *The boundaries of the West African Craton*. Geological Society of London Special Publication, 297 (pp. 385–408). https://doi.org/10.1144/SP297.18.

Pereira, M. F., El Houicha, M., Chichorro, M., Armstrong, R., Jouhari, A., El Attari, A., et al. (2015). Evidence of a Paleoproterozoic basement in the Moroccan Variscan Belt (Rehamna Massif, Western Meseta). *Precambrian Research, 268,* 61–73. https://doi.org/10.1016/j.precamres.2015.07.010.

Pereira, M.F., Gama, C., Dias da Silva, I., Fuenlabrada, J.M., Brandão Silva, J. & Medina, J., (2020). Isotope geochemistry evidence for Laurussian-type sources of South-Portuguese Zone Carboniferous turbidites (Variscan orogeny) Geological Society, London, Special Publications, 503. https://doi.org/10.1144/SP503-2019-163.

Pereira, M. F., Linnemann, U., Hofmann, M., Chichorro, M., Solá, A. R., Medina, J., & Silva, J. B. (2012a). The provenance of Late Ediacaran and Early Ordovician siliciclastic rocks in the Southwest Central Iberian Zone: Constraints from detrital zircon data on northern Gondwana margin evolution during late Neoproterozoic. *Precambrian Research, 192–195,* 166–189. https://doi.org/10.1016/j.precamres.2011.10.019.

Pereira, M. F., Solá, A. R., Chichorro, M., Lopes, L., Gerdes, A., & Silva, J. B. (2012b). North Gondwana assembly, break-up and paleogeography: U–Pb isotope evidence from detrital and igneous zircons of Ediacaran and Cambrian rocks of SW Iberia. *Gondwana Research, 22*(3–4), 866–881. https://doi.org/10.1016/j.gr.2012.02.010.

Pérez Estaún, A., Bea, F., Marcos, A., Martínez Catalán, J.R., Martínez Poyatos, D., Arenas, R., Díaz García, F., Azor, A., Simancas, F. & González Lodeiro, F., (2004). In J.A. Vera, (Ed.) *La cordillera varisca europea: el Macizo ibérico En: Geología de España* (pp. 21–25) Madrid: SGE-IGME.

Pieren Pidal, A.P., (2000). Las sucesiones anteordovícicas de la región oriental de la provincial de Badajoz y área contigua de la de Ciudad Real. Thesis Universidad Complutense Madrid, Ph.D (pp. 379).

Quesada, C., (1990). Precambrian successions in SW Iberia: their relationships to Cadomian orogenic events. In R.S D'Lemos, R.A. Strachan & C.G. Topley (Eds.), *The Cadomian Orogeny* (pp. 353–362) Geological Society London, Special Publication 51. https://doi.org/10.1144/GSL.SP.1990.051.01.23.

Quesada, C., Apalategui, O., Eguiluz, L., Liñán, E., & Palacios, T. (1990). Ossa-Morena zone: precambrian. In R. D. Dallmeyer & E. Martínez-García (Eds.), *Pre-mesozoic geology of Iberia* (pp. 250–258). Berlin: Springer.

Ribeiro, A., Munhá, J., Dias, R., Mateus, A., Pereira, E., Ribeiro, L., Fonseca, P., Araújo, A., Oliveira, T., Romão, J., Chaminé, H., Coke, C. & Pedro, J., (2007). Geodynamic evolution of the SW Europe Variscides. *Tectonics*, *26*, TC6009. https://doi.org/10.1029/2006TC002058.

Ries, A. C., & Shackleton, R. M. (1971). Catazonal complexes of north-west Spain and north Portugal, remnants of a Hercynian thrust plate. *Nature Physical Science, 234,* 65–68. https://doi.org/10.1038/physci234065a0.

Robardet, M., (1976): L'originalité du segment hercynien sudibérique au Paléozoïque inférieur: Ordovicien, Silurien et Dévonien dans le nord de la province de Séville (Espagne). Comptes Rendus de l'Académie des Sciences, Paris, 283, série D (pp. 999–1002).

Rodríguez Alonso, M.D., Díez Balda, M.A., Perejón, A., Pieren, A., Liñán, E., López Díaz, F., Moreno, F., Gámez Vintaned, J.A., González Lodeiro, F., Martínez Poyatos, D. & Vegas, R., (2004a). Dominio del Complejo esquisto-grauváquico. Estratigrafía. La secuencia litoestratigráfica del Neoproterozoico–Cámbrico inferior. In J.A Vera (Ed.), *Geología de España*. Sociedad Geológica de España-Instituto Geológico y Minero de España, Madrid, (pp. 78–81).

Rodríguez Alonso, M. D., Peinado, M., López-Plaza, M., Franco, P., Carnicero, A., & Gonzalo, J. C. (2004b). Neoproterozoic-Cambrian synsedimentary magmatism in the Central Iberian Zone (Spain): Geology, petrology and geodynamic significance. *International Journal of Earth Sciences, 93,* 897–920. https://doi.org/10.1007/s00531-004-0425-4.

Rojo-Pérez, E., Arenas, R., Fuenlabrada, J. M., Sánchez Martínez, S., Martín Parra, L. M., Matas, J., et al. (2019). Contrasting isotopic sources (Sm–Nd) of Late Ediacaran series in the Iberian Massif: Implications for the Central Iberian–Ossa Morena boundary. *Precambrian Research, 324,* 194–207. https://doi.org/10.1016/j.precamres.2019.01.021.

Rojo-Pérez, E., Fuenlabrada, J.M., Linnemann, U., Arenas, R., Sánchez Martínez, S., Díez Fernández, R., Martín Parra, L.M., Matas, J., Andonaegui, P. & Fernández-Suárez, J., (submitted). Geochemistry and Sm–Nd isotopic sources of Late Ediacaran siliciclastic series in the Ossa-Morena Complex: Iberian-Bohemian correlations. *International Journal of Earth Sciences*.

Rubio Pascual, F. J., Matas, J., & Martín Parra, L. M. (2013). High-pressure metamorphism in the Early Variscan subduction complex of the SW Iberian Massif. *Tectonophysics, 592,* 187–199. https://doi.org/10.1016/j.tecto.2013.02.022.

San José, M. A., Pieren, A. P., García Hidalgo, F. J., Vilas, L., Herranz, P., Peláez, J. R., & Perejón, A. (1990). Central Iberian Zone: Ante-Ordovician stratigraphy. In R. D. Dallmeyer & E. Martínez García (Eds.), *Pre-Mesozoic Geology of Iberia* (pp. 147–159). Berlin Heidelberg New York: Springer.

Sánchez Carretero, R., Carracedo, M., Eguíluz, L., & Apalategui, O. (1989). El magmatismo calcoalcalino del Precámbrico terminal en la Zona de Ossa-Morena (Macizo Ibérico). *Revista de la Sociedad Geológica de España, 2,* 7–21.

Sánchez García, T., Quesada, C., Bellido, F., Dunning, G. R., & González del Tánago, J. (2008). Two-step magma flooding of the upper crust during rifting: The Early Paleozoic of the Ossa Morena Zone (SW Iberia). *Tectonophysics, 461,* 72–90. https://doi.org/10.1016/j.tecto.2008.03.006.

Sánchez Martínez, S., Arenas, R., Albert, R., Gerdes, A. & Fernández-Suárez, J., (2020) Updated geochronology and isotope geochemistry of the Vila de Cruces Ophiolite: A case study of a peri-Gondwanan back-arc ophiolite. Geological Society, London, Special Publications, 503. https://doi.org/10.1144/SP503-2020-8.

Sánchez-García, T., Chichorro, M., Solá, A.R., Álvaro, J.J., Díez-Montes, A., Bellido, F., Ribeiro, M.L., Quesada, C., Lopes, J.C., Dias da Silva, Í., González-Clavijo, E., Gómez Barreiro, J. & López-Carmona, A., (2019). The Cambrian-Early Ordovician Rift Stage in the Gondwanan Units of the Iberian Massif. In C. Quesada & J. Oliveira (Eds), *The Geology of Iberia: A Geodynamic Approach*. Regional Geology Reviews. Cham: Springer. https://doi.org/10.1007/978-3-030-10519-8_2.

Sánchez-García, T., Pereira, M. F., Bellido, F., Chichorro, M., Silva, J. B., Valverde-Vaquero, P., et al. (2014). Early Cambrian granitoids of North Gondwana margin in the transition from a convergent setting to intra-continental rifting (Ossa-Morena Zone, SW Iberia). *International Journal of Earth Sciences (Geol Rundsch), 103,* 1203–1218. https://doi.org/10.1007/s00531-013-0939-8.

Schäfer, H.-J., Gebauer, D., Nägler, T. F., & Eguiluz, L. (1993). Conventional and ion-microprobe U–Pb dating of detrital zircons of the Tentudía Group (Serie Negra, SW Spain): Implications for zircon systematics, stratigraphy, tectonics and the Precambrian/Cambrian boundary. *Contributions to Mineralogy and Petrology, 113*(3), 289–299. https://doi.org/10.1007/BF00286922.

Simancas, J. F., Azor, A., Martínez-Poyatos, D., Tahiri, A., El Hadi, H., González-Lodeiro, F., et al. (2009). Tectonic relationships of Southwest Iberia with the allochthons of Northwest Iberia and the Moroccan Variscides. *Comptes Rendus Geoscience, 341,* 103–113. https://doi.org/10.1016/j.crte.2008.11.003.

Simancas, J. F., Galindo-Zaldivar, J., & Azor, A. (2000). Three-dimensional shape and emplacement of the Cardenchosa deformed pluton (Variscan Orogen, southwestern Iberian Massif). *Journal of Structural Geology, 22*(4), 489–503.

Stampfli, G. M., Hochard, C., Vérard, C., Wilhem, C., & von Raumer, J. (2013). The formation of Pangea. *Tectonophysics, 593,* 1–19. https://doi.org/10.1016/j.tecto.2013.02.037.

Stampfli, G.M., von Raumer, J. & Borel, G.D., (2002). Paleozoic evolution of pre-Variscan terranes: from Gondwana to the Variscan collision. In J.R Martínez Catalán, R.D. Hatcher Jr., R. Arenas & F. Díaz García, (Eds.), *Variscan-Appalachian Dynamics: The Building of the Late Paleozoic Basement*. Geological Society of America Special Paper vol. 364, (pp. 263–280). https://doi.org/10.1130/0-8137-2364-7.263.

Stephan, T., Kroner, U., & Romer, R. L. (2019b). The pre-orogenic detrital zircon record of the Peri-Gondwanan crust. *Geological Magazine, 156*(2), 281–307. https://doi.org/10.1017/S0016756818000031.

Stephan, T., Kroner, U., Romer, R. L., & Rösel, D. (2019a). From a bipartite Gondwanan shelf to an arcuate Variscan belt: The early Paleozoic evolution of northern Peri-Gondwana. *Earth-Science Reviews, 192,* 491–512. https://doi.org/10.1016/j.earscirev.2019.03.012.

Stern, R. J. (2002). Crustal evolution in the East African Orogen: A neodymium isotopic perspective. *Journal of African Earth Sciences, 34*(3–4), 109–117. https://doi.org/10.1016/S0899-5362(02)00012-X.

Talavera, C., Montero, P., Bea, F., González Lodeiro, F., & Whitehouse, M. (2013). U–Pb Zircon geochronology of the Cambro–Ordovician metagranites and metavolcanic rocks of central and NW Iberia. *International Journal of Earth Sciences, 102,* 1–23. https://doi.org/10.1007/s00531-012-0788-x.

Talavera, C., Montero, P., Martínez Poyatos, D., & Williams, I. S. (2012). Ediacaran to Lower Ordovician age for rocks ascribed to the Schist–Graywacke Complex (Iberian Massif, Spain): Evidence from detrital zircon SHRIMP U–Pb geochronology. *Gondwana Research, 22,* 928–942. https://doi.org/10.1016/j.gr.2012.03.008.

Tanaka, T., Togashi, S., Kamioka, H., Amakawa, H., Kagami, H., Hamamoto, T., et al. (2000). JNdi-1: A neodymium isotopic reference in consistency with La Jolla neodymium. *Chemical Geology, 168,* 279–281. https://doi.org/10.1016/S0009-2541(00)00198-4.

Taylor, S.R. & McLennan, S.M., (1985). The Continental Crust: Its Composition and Evolution. Blackwell, Oxford (pp. 312). ISBN-13: 978-0632011483.

Taylor, S.R. & McLennan, S.M., (1988). The significance of the rare earths in geochemistry and cosmochemistry, Handbook on the Physics and Chemistry of Rare Earths, Elsevier, Vol 11, (pp. 485–578). ISSN 0168-1273, ISBN 9780444870803. https://doi.org/10.1016/S0168-1273(88)11011-8.

Ugidos, J. M., Billström, K., Valladares, M. I., & Barba, P. (2003a). Geochemistry of the Upper Neoproterozoic and Lower Cambrian siliciclastic rocks and U–Pb dating on detrital zircons in the Central Iberian Zone, Spain. *International Journal of Earth Sciences, 92,* 661–676. https://doi.org/10.1007/s00531-003-0355-6.

Ugidos, J. M., Valladares, M. I., Barba, P., & Ellam, R. M. (2003b). The Upper Neoproterozoic-Lower Cambrian of the Central Iberian Zone, Spain: Chemical and isotopic (Sm–Nd) evidence that the sedimentary succession records an inverted stratigraphy of its source. *Geochimica et Cosmochimica Acta, 67,* 2615–2629. https://doi.org/10.1016/S0016-7037(03)00027-9.

Valladares, M. I., Barba, P., Ugidos, J. M., Colmenero, J. R., & Armenteros, I. (2000). Upper Neoproterozoic-Lower Cambrian sedimentary successions in the Central Iberian Zone (Spain): Sequence stratigraphy, petrology and chemostratigraphy. Implications for other European zones. *International Journal of Earth Sciences, 89,* 2–20.

Valladares, M. I., Ugidos, J. M., Barba, P., & Colmenero, J. R. (2002). Contrasting geochemical features of the Central Iberian Zone shales (Iberian Massif, Spain): Implications for the evolution of Neoproterozoic-Lower Cambrian sediments and their sources in other Peri-Gondwanan areas. *Tectonophysics, 352,* 121–132. https://doi.org/10.1016/S0040-1951(02)00192-0.

Villaseca, C., Merino, E., Oyarzun, R., Orejana, D., Pérez-Soba, C., & Chicharro, E. (2014). Contrasting chemical and isotopic signatures from Neoproterozoic metasedimentary rocks in the Central Iberian Zone (Spain) of pre-Variscan Europe: Implications for terrane analysis and Early Ordovician magmatic belts. *Precambrian Research, 245,* 131–145. https://doi.org/10.1016/j.precamres.2014.02.006.

von Raumer, J. F., Stampfli, G. M., Borel, G. D., & Bussy, F. (2002). The organization of pre-Variscan basement areas at the Gondwana margin. *International Journal of Earth Sciences, 91,* 35–52. https://doi.org/10.1007/s005310100200.

von Raumer, J. F., Stampfli, G. A., & Bussy, F. (2003). Gondwana-derived microcontinents—the constituents of the Variscan and Alpine collisional orogens. *Tectonophysics, 365,* 7–22. https://doi.org/10.1016/S0040-1951(03)00015-5.

Whitney, D. L., & Evans, B. W. (2010). Abbreviations for names of rock forming minerals. *American Mineralogist, 95,* 185–187. https://doi.org/10.2138/am.2010.3371.

Winchester, J. A., & Floyd, P. A. (1977). Geochemical discrimination of different magma series and their differentiation products using immobile elements. *Chemical Geology, 20,* 325–343. https://doi.org/10.1016/0009-2541(77)90057-2.

Winchester, J. A., & Max, M. D. (1989). Tectonic setting discrimination in clastic sequences: An example from the late proterozoic Erris Group, NW Ireland. *Precambrian Research, 45*(1–3), 191–201. https://doi.org/10.1016/0301-9268(89)90039-9.

Winchester, J.A., Pharaoh, T.C. & Verniers, J., (2002). Palaeozoic amalgamation of Central Europe: An introduction and synthesis of new results from recent geological and geophysical investigations. In J.A. Winchester, T.C. Pharaoh & J. Verniers (Eds.), *Palaeozoic Amalgamation of Central Europe*. Geological Society, London, Special Publications vol. 201, (pp. 1–18). https://doi.org/10.1144/GSL.SP.2002.201.01.01.

Zhao, J. X., McCulloch, M. T., & Bennett, V. C. (1992). Sm–Nd and U–Pb zircon isotopic constraints on the provenance of sediments from the Amadeus Basin, central Australia: Evidence for REE fractionation. *Geochimica et Cosmochimica Acta, 56*(3), 921–940. https://doi.org/10.1016/0016-7037(92)90037-J.

Affiliations

José Manuel Fuenlabrada[1] · Ricardo Arenas[2] · Rubén Díez Fernández[3] · José González del Tánago[2] · Luis Miguel Martín-Parra[3] · Jerónimo Matas[3] · Esther Rojo-Pérez[2] · Sonia Sánchez Martínez[2] · Pilar Andonaegui[2] · Byron Solis Alulima[2]

Ricardo Arenas
rarenas@ucm.es

Rubén Díez Fernández
r.diez@igme.es

José González del Tánago
tanago@geo.ucm.es

Luis Miguel Martín-Parra
lm.martin@igme.es

Jerónimo Matas
j.matas@telefonica.net

Esther Rojo-Pérez
e.rojo@ucm.es

Sonia Sánchez Martínez
s.sanchez@geo.ucm.es

Pilar Andonaegui
andonaeg@geo.ucm.es

Byron Solis Alulima
bysolis@ucm.es

[1] Unidad de Geocronología (CAI de Ciencias de la Tierra y Arqueometría), Universidad Complutense de Madrid, Facultad de Ciencias Geológicas, Calle José Antonio Novais 12, 28040 Madrid, Spain

[2] Departamento de Mineralogía y Petrología e Instituto de Geociencias (UCM, CSIC), Universidad Complutense, Madrid, Spain

[3] Instituto Geológico y Minero de España, Tres Cantos, 28760 Madrid, Spain